Bio-based aviation fuel production

A techno-economic viability analysis of producing BTX from biomass.

KE2325 Process Design for Industry and Society

Akshay Menon[1], Alex Mosquera[2], Johannes Johansson[3], M. Carmen Aliques[4], Nima Mirzaei[5], Robert Dahl[6], Samuel af Ugglas[7], Soumia Amara[8]

Supervisors: Efthymios Kantarelis and Klas Engvall

12 December 2019

KTH Royal Institute of Technology

Stockholm, Sweden

[1]akshayme@kth.se, [2]alexmo@kth.se, [3]jjo9@kth.se, [4]mdcat@kth.se, [5]nmirzaei@kth.se, [6]rodah@kth.se, [7]samuelau@kth.se, [8]soumiaa@kth.se

Abstract

In this study, a process was developed for production of benzene, toluene and xylene (BTX) for jet-fuel, using biomass as raw material as an alternative to the present production which is based on fossil fuel. The initial proposed design was gasification of biomass with a higher heating value (HHV) of $50\ MW$ configured to maximize BTX production, followed by appropriate separation and conditioning processes to extract a relatively pure mixture of BTX. The remaining energy gas produced in the gasification would be sent to a combined heat and power (CHP) process to provide district heating and power as a secondary goal.

In the final design of the process, the biomass chosen was chosen as wood chips from Värnamo. This would first be processed in a shredder followed by a drier as pre-treatment for gasification. A circulating fluidized bed (CFB) technology with silica sand was chosen for the gasifier, using air as the gasifying agent, and the produced gas phase mixture would be sent to a tar cracker. A fluid catalytic cracking (FCC) technology was chosen for the tar cracker, with a catalyst found selective to benzene formation. The remaining tar compounds excluding BTX, i.e. aromatics such as naphthalene, would then be absorbed by using triethylene glycol (TEG) in a scrubber, and the TEG would subsequently be regenerated in distillation unit, and the remaining tar would be recirculated to the tar cracker. The remaining mixture of energy gas and BTX would then be sent to an adsorption column filled with activated carbon. Here the BTX would be adsorbed selectively, and after subsequent desorption a relatively pure mixture of BTX would be acquired. The remaining BTX-free energy gas would be sent to a boiler, and the heat from combustion would be used to heat a steam cycle. The heated steam would be sent through a turbine to produce power, and the remaining heat would be extracted and sold as district heating.

After choosing operating conditions, performing mass and energy balances over each unit process as well as an overall economic analysis, the net present value (NPV) was found to not be positive until after 15 years of operation. It was concluded that the present process would not be a feasible investment, but several suggestions for further improvements were provided. In general, the gasifier should be optimized further for BTX production through a laboratory study, the overall system might be pressurized to allow the use of a more effective catalyst in the tar cracker as well as reduce the demand on the separation processes, and the formed biochar and coke could be burned to further increase the energy production. If the demand of renewable BTX also increased over time, with a higher sale price, the process might then prove to be more profitable.

Table 1 – Abbreviations used throughout the paper

1-PhO	1-Phenyloctane
9,10-DHP	9,10-dihydrophenanthrene
AC	Activated Carbon
BaA	Benzanthrazene
BFB	Bubbling Fluidized Bed
BP	Boiling Point
BTX	Benzene, Toluene, Xylene
CFB	Circulating Fluidized bed
CHP	Combined Heat and Power
DAF	Dry and Ash-Free
DEG	Diethylene Glycol
ER	Equivalent Ratio
FCC	Fluid Catalytic Cracking
FGC	Flue Gas Condenser
FFP	Fit-For-Purpose
GA	Gasifying Agent
GHG	Greenhouse Gas
GROT	"Grenar och (Träd)Toppar" (branches and tree-tops)
HHV	Higher Heating Value
LHV	Lower Heating Value
LLE	Liquid-Liquid Extraction
Nm^3	Normal cubic meter, defined at $0℃$ and $1\ atm$
NPV	Net Present Value
RME	Rapeseed-Methyl-Ester
TEG	Tri-Ethylene Glycol
VOC	Volatile Organic Compounds
ROI	Return on Investment
FCI	Fixed Capital Investment
WCI	Working Capital Investment
TCI	Total Capital Investment

Table 2 – Nomenclature used throughout the paper

$\Delta_f H^\circ$	Specific heat of formation at 25°C $(kJ/mol.K)$
$\Delta_{fus} H^\circ$	Specific heat of fusion at 25°C $(kJ/mol.K)$
$\Delta_{Rx} H^\circ$	Specific heat of reaction at 25°C $(kJ/mol.K)$
$\Delta_{sub} H^\circ$	Specific heat of sublimation at 25°C $(kJ/mol.K)$
$\Delta_{vap} H^\circ$	Specific heat of vaporization at 25°C $(kJ/mol.K)$
$c_{p,i}$	Specific heat capacity of component i $(kJ/mol.K)$
ΔH_s	Isosteric heat of desorption (kJ/mol)
$H\{t,p\}$	Specific enthalpy at temperature T and pressure p (kJ/kg)
ρ	Density (kg/m^3)
p	Pressure (Pa)
T	Temperature $(K\ or$ °C)
R	Ideal gas constant $(8.314\ Pa.m^3/mol.K)$
V	Volume (m^3)
A	Area (m^2)
d	Diameter (m)
$E_{k,i}$	Energy of component i in stream k (MW)
$F_{k,i}$	Mass flow of component i in stream k $(kg/s)\ or\ (kg/h)$
M_i	Molecular weight of component i (g/mol)
n_i	Moles of component i (mol)
$\dot{n}_i$	Molar flows of component i (mol/h)
$P_{k,j,i}$	Production of component i in unit j from stream k (kg/s)
r	Discount rate (%)
r_i	Inflation rate (%)
x_i	Molar fraction of component i in dry and tar-free content of stream S4
X_i	Conversion of component i
S_i	Selectivity of component i
τ	Residence time (s)
v	Volumetric flow (m^3/s)
h	Height (m)
p_w	Vapor pressure of water (mmHg)
x_p	Biomass particle thickness (inch)
W	Average moisture content $(\%)$
W_e	Equilibrium moisture content $(\%)$
W_0	Initial moisture content $(\%)$
m	Mass (kg)
$X_{M,i}$	Initial moisture content of biomass $(kg/kg_{dry\ basis})$
$X_{M,f}$	Final moisture content of biomass $(kg/kg_{dry\ basis})$
r_0	Latent heat of evaporation of water $(\mathrm{kJ/kg})$
T_D	Drying temperature (K)
T_0	Ambient air temperature (K)
F_a	Flow rate of air required to dry biomass $(\mathrm{kg/s})$
Y_0	Ambient air humidity $(\%)$
ΔY	Humidity difference $(\%)$

Contents

1 Introduction

The use of renewable resources is becoming increasingly important in the attempts to minimize greenhouse gas (GHG) emission. In order to replace the current fossil fuels, one promising option is the production of biofuels from biomass [1]. For the aviation section, GHG emissions are rapidly growing. According to the European Commission, direct emissions from aviation bear responsibility for 3% of the EU's total GHG emissions and more than 2% of the global emissions. Moreover, the European Commission announced that the global international aviation emissions by 2020 will be 70% higher than in 2005 [2].

Bio-based aviation fuel production is one of the proposed solutions to reduce GHG emission. A conventional aviation fuel contains several types of hydrocarbons, such as normal and iso-paraffins, cyclo-paraffins and aromatics [3]. The aromatics fraction is a mixture of benzene, toluene and xylene (BTX) comprising 20-25% of the fuel [4]. In petroleum refining and petrochemical industries, BTX is recovered from the catalytic reforming of naphtha [5].

Bio-BTX have identical molecules to their fossil fuel-based counterparts. Apart from providing energy to the jet engine, the main purpose of adding BTX to the jet fuel is its material compatibility which provides a significant thermal stability and increases seal swell capacity and volume [6]. Thus, replacing BTX produced from fossil fuels with the renewable BTX could play an important role in the reduction of GHG emission from aviation due to the carbon neutrality of biomass-based fuels. Moreover, it is possible to save up 80% in CO_2 emissions through the aircraft's life cycles, by using bio-aviation fuels [4].

BTX is proposed to be produced by a conditioning separation process for the producer gas from biomass gasification enriched tar production. Tar is generally a mixture of a wide range of aromatic compounds, part of it being BTX. With the appropriate separation processes, the BTX could be extracted from the gas and tar mixture to then be added to jet fuel for the intent of providing the material compatibility above explained. The energy gas could be used for combined heat and power (CHP) production. The suggested system is shown in Figure 1.

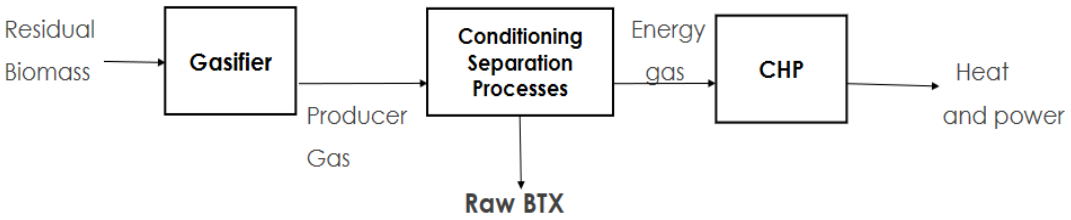

Figure 1 – Process of BTX production from conditioned tar

1.1 Scope of the project and outline

The main objective of this study was to design a process for BTX production according to the system shown above based on an inlet of 50 MW. This was to be done following the principles of green chemistry, with the main goal of maximizing the production of BTX, and a secondary goal of producing power and district heating.

This paper starts with some background relevant for the process before going into more detail of the process design. The process design section shows some of the technologies and operational conditions

considered for the different units together with motivations for the chosen processes. Next, the mass and energy balances are presented for each chosen unit along with assumptions made in the calculations, and summaries of the final results. Lastly, an economic evaluation of the entire process and ultimately a discussion of the results, impact of assumptions and choices made, the economic viability of the process and possible improvements. The performed calculations in detail are shown in the appendix.

2 Background

2.1 Biomass

Biomass is an organic renewable source of energy which can be harvested from various sources such as animals, agricultural and forestry residues or even municipal solid waste, as shown in Figure 2. Biomass as a source of energy can be an environmental-friendly alternative to fossil fuel-based sources. Biomass used for the production of biofuels and heat benefits from zero emissions of GHG to the atmosphere [7].

Figure 2 - Sources of biomass [7]

The biomass could be classified into different categories, depending on their properties, as follows [7]:

- Wood and woody biomass
- Herbaceous plants/grasses
- Aquatic plants
- Animal manure and human sewage

The woody biomass, which include many materials such as trees, shrubs and bushes among others, could be burned directly to produce energy or be converted into a liquid or gas by different conversion processes [7].

Herbaceous plants could be subdivided based on their moisture content [8]. This category contains materials such as non-woody plants, cereals and grains, which could be burned as a fuel or also be converted to liquid biofuels [9].

Aquatic biomass are high-moisture materials such as microalgae, macroalgae and emerging plants [8]. The amount of biomass obtained from these raw materials is less than that of woody biomass or herbaceous plant. However, these materials present the ability to convert water, sunlight and CO_2 into algal biomass [7].

Another type of directly for heating biomass is the animal manure and human sewage, which includes materials such as bones, meat meal and different types of animal manures. Through anaerobic

digestion useful products such as biogas are obtained, which could be burned for energy. Moreover, this raw material could be burned directly for district heating [7].

The properties of the biomass determine the conversion process to obtain useful products, as well as the difficulties of carrying out the conversion process. The main properties of biomass are the moisture content, the calorific value, the proportions of fixed carbon and volatiles, the ash or residue content, the alkali metal content and the cellulose/lignin ratio [8].

Moisture content is a characteristic of high importance for biomass, in order to prevent possible impacts that deteriorate the material during the treatment and processing process, as well as in the transport and storage of biomass. Raw materials with low moisture are the most suitable for thermal conversions, and the materials with high moisture content are more efficient in producing useful products by biochemical conversion [8].

2.2 Pre-treatment of biomass

The object in this part of the process is to treat the biomass fed into the plant, to render it fit for further treatment downstream. For this purpose, the biomass with non-homogeneous particle sizes are chipped and grinded in a shredder to homogenize the particles. The shredder is provided with a grate at its exit to screen the particles and to ensure uniform size-distribution.

As mentioned previously, the biomass fed into the plant contains significant amount of moisture, and therefore, drying the biomass and reducing its moisture content will be a necessity. It is also reported that a lower amount of bound moisture has the ability to increase the adiabatic flame temperature in the subsequent gasification stage. This is supported by the fact that higher amount of energy will be used during gasification to evaporate the residual water content, and thus, lower packets of energy will be utilized for effective gasification [10]. A rotary single-pass air blown drier is a good option for this purpose. Detailed description about the drying stages can be found in section 3.2.2.

2.3 BTX

Benzene, toluene and xylene (BTX), are aromatic compounds of high importance in industry, particularly for chemical processes. They are the base material for production of petrochemicals, chemicals, solvents or fuels [11]. Moreover, the mixture of these aromatic compounds is also used as a feedstock for benzene extraction, used in many industrial applications, e.g. production of plastics, detergents or pesticides. Once the benzene is extracted, the other components of the mixture will be separated into toluene, which could be used to produce solvents and be added to gasolines with high octane number. The xylene used for instance as solvent or cleaning agent [11] [12]. Their molecular structures are shown in Figure 3.

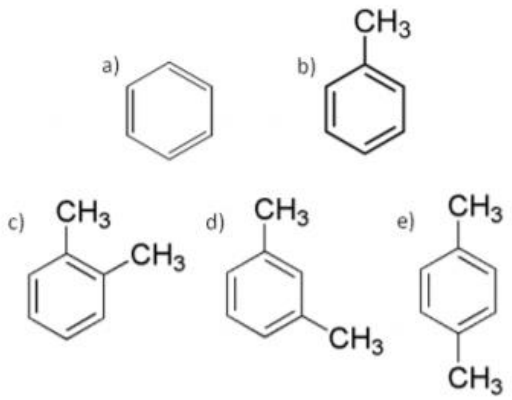

Figure 3 – Molecular structures of a) Benzene, b) Toluene, c) Ortho-xylene, d) meta-xylene and e) para-xylene [13]

The current production of BTX has harmful impacts on the environment, as it is typically produced from petrochemical processes using fossils fuels [13]. Even so, according to a new economic study conducted by Ajay More, the global market for aromatic compounds is in continuous growth, and a growth of 7.5 % in the next five years is expected [14].

An alternative way of BTX production is necessary, in order to reduce its current environmental impacts and to keep-up with the increasing demand of BTX production at the same time. One alternative, as was explored in this project, could be to gasify biomass instead of exert fossil fuels to produce BTX and potentially reduce emissions of compounds such as NO_X, SO_X and CO_2 [13].

2.4 Biomass gasification

Gasification of biomass is a process used to convert the biomass into gases without combustion, which could later be used in many processes, in gas engines or gas turbines in order to generate electricity [15]. Gasification is performed in a reactor called gasifier, and the overall process and products are summarized in Figure 4. The gas obtained in this process mainly consists of a mixture of H_2, CO, CO_2 and H_2O, and N_2 if air is supplied, as well as light hydrocarbons such as CH_4 and some C_2-C_3 [16] [17].

The conversion of biomass occurs by using a gasifying agent (GA) such as air, steam, pure oxygen, a mixture of those or carbon dioxide [18]. In the case of air as the gasifying agent, N_2 generally acts as inert and its only effect is the dilution of the product gas. In addition to the gas phase, ash and char will form as solids. Char is a product of incomplete gasification typically considered to be pure carbon, while ash generally is the solid compounds that would remain after combustion of biomass [17].

The product distribution from the gasifier is a function of the process variables, including temperature, oxygen and steam injection, pressure, residence time, the composition of biomass and the gasification technology [18]. The temperature of a gasification process is generally around $800-900$ ℃ [8].

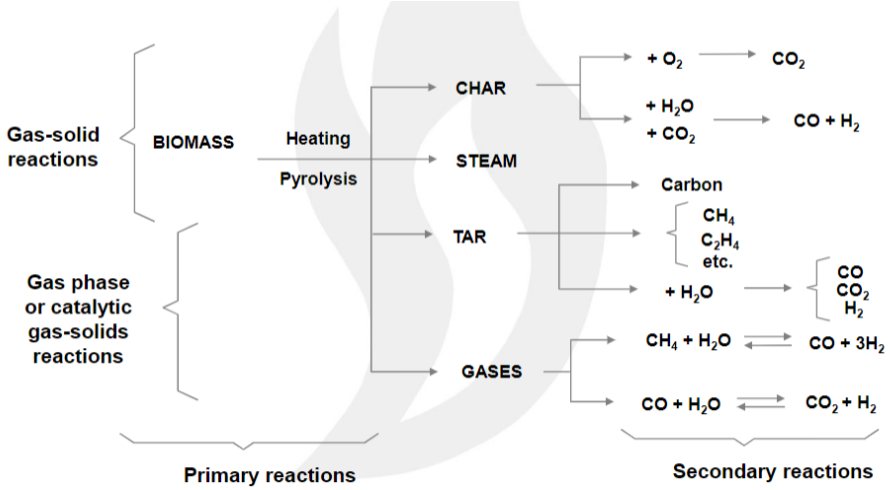

Figure 4 – Reaction scheme of gasification process [19]

In accordance with Figure 4, the primary reactions occurring in the biomass gasification are the pyrolysis reactions, where char, steam, tar and gases are generated by heating, occurring in the absence of a gasifying agent. Tar is a complex mixture of hydrocarbons, discussed in more detail in section 2.5. This is followed by several secondary reactions which form mainly syngas, a mixture of CO and H_2 from the gases, liquids and solids previously produced. The main reactions involve carbon oxides, hydrogen, water and methane, and are summarized below.

1. Reactions with molecular oxygen [20].

$$C + {}^{1}/_{2}\,O_2 \rightarrow CO \qquad \Delta H = -111\ \mathrm{kJ/mol} \qquad (1)$$

$$CO + {}^{1}/_{2}\,O_2 \rightarrow CO_2 \qquad \Delta H = -283\ \mathrm{kJ/mol} \qquad (2)$$

$$H_2 + {}^{1}/_{2}\,O_2 \rightarrow H_2O \qquad \Delta H = -242\ \mathrm{kJ/mol} \qquad (3)$$

2. Boudouard reaction [20].

$$C + CO_2 \leftrightarrow 2CO \qquad \Delta H = +172.54\ \mathrm{kJ/mol} \qquad (4)$$

3. Reaction with steam, the heterogeneous water-reaction [20].

$$C + H_2O \leftrightarrow H_2 + CO \qquad \Delta H = +131.38\ \mathrm{kJ/mol} \qquad (5)$$

4. Reaction with hydrogen, the methanation reaction [20].

$$2H_2 + C \leftrightarrow CH_4 \qquad \Delta H = -75\ \mathrm{kJ/mol} \qquad (6)$$

5. Water-gas shift reaction [20].

$$CO + H_2O \leftrightarrow CO_2 + H_2 \qquad \Delta H = -41\ \mathrm{kJ/mol} \qquad (7)$$

6. Steam-methane reforming reaction [20].

$$CH_4 + H_2O \leftrightarrow CO_2 + 3H_2 \qquad \Delta H = +206\ \mathrm{kJ/mol} \qquad (8)$$

2.5 Tar

As mentioned previously, the biomass gasification process comprises of pyrolysis and oxidation reactions in condensed and vapor phases. A variety of organic compound are formed during this process, depending also on the gasifying conditions, such as temperature, pressure, residence time or addition of air and steam [21].

One of the products of gasification, tar, condenses at low temperatures to form a black thick viscous liquid, which might lead to clogging of the system [22]. The formation of tar increases operational problems due to formation of coke, causing condensation at cold spots and cracks on the filters [23]. However, there is no universally accepted definition of which compounds count as tar and which ones does not. Hence, there are differences between the sources regarding the nature of tar [22].

One definition considers tar as the mixture of condensable products formed during gasification, including aromatic compounds and polycyclic aromatic hydrocarbons (PAHs) [21] [24]. The most established definition assumes tar to be aromatics heavier than benzene [25]. Figure 5 shows the transition of tar compounds formed in the gasifier depending on the temperature, as proposed by Elliot [26]. In this report, tar was considered as benzene and any aromatic compounds heavier than it.

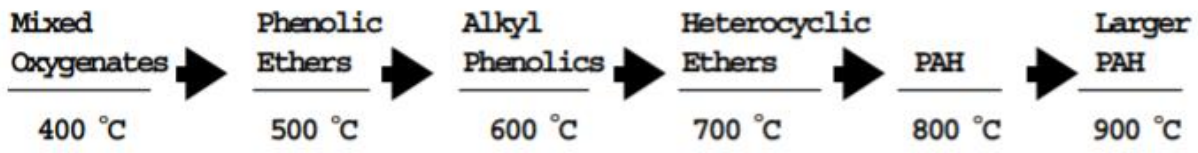

Figure 5 – Transition of tar as a function of process temperature [26]

A typical composition of biomass tars is shown in Table 3. In truth, this composition depends on the process conditions, the type of gasifier and even the feed material to the gasifier [24].

Table 3 – Typical composition of tar [22]

Component	Weight (%)
Benzene	37.9
Toluene	14.3
Other 1-ring aromatic hydrocarbons	13.9
Naphthalene	9.6
Other 2-ring aromatic hydrocarbons	7.8
3-ring aromatic hydrocarbons	3.6
4-ring aromatic hydrocarbons	0.8
Phenolic compounds	4.6
Heterocyclic compounds	6.5
Others	1.0

Other than BTX, the model tar compounds for this project are shown in Figure 6. These compounds correspond to the used reactants in the experiments conducted by Pujro et al. [27]. When required, the tar was assumed to be only composed of BTX and naphthalene, where naphthalene replaced all the neglected compounds.

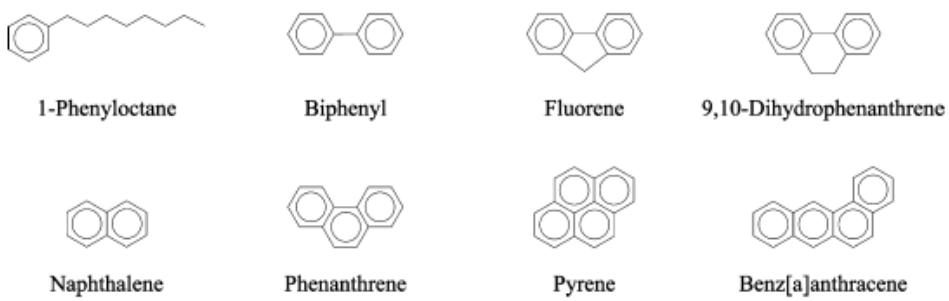

Figure 6 – Model tar compounds [27]

To approximate the composition of tar, the model tar compounds were compared and distributed according to Table 3, then normalized to compensate for the sections of tar not in the model. Table 4 lists the weight fractions of the model tar used for this project.

Table 4 – Composition of model tar

Model Tar Compounds	**Weight fraction** (%)
1-PhO	10.458
Biphenyl	3.055
Fluorene	3.055
9,10-DHP	3.055
Naphthalene	10.576
Phenanthrene	4.230
Pyrene	0.470
Benzanthracene	0.470
Benzene	47.004
Toluene	11.751
Xylene	5.875

2.6 Gasification technologies

Gasifiers generally vary in the way the biomass and the gasifying agent are put in contact and mixed, which leads to different transfer rates, residence times as well as product compositions [15]. Some available technologies are fixed bed, entrained flow and fluidized bed gasifiers.

Fixed bed gasifiers are classified as updraft or downdraft. In updraft, biomass is introduced at the top of the gasifier and the gasifying agent at the bottom, while in downdraft, both biomass and gasifying agent are supplied at the top. While fixed bed gasifiers can produce high tar contents, they are only applicable to small-scale operations, below $10\ MW$ [17].

In entrained-flow gasifiers, both air flow and biomass are introduced from the top of the equipment as it appears in Figure 7. The operating temperature is higher than 1200 ℃. The reactor operates at such high temperatures due to short resident time and to maintain high conversions. Moreover, the operating pressure is often 20-80 bar. This type of gasifier is most suitable if the BTX were to be produced only from syngas because the producer gas produced in this reactor contains mostly only syngas and almost no tar [28].

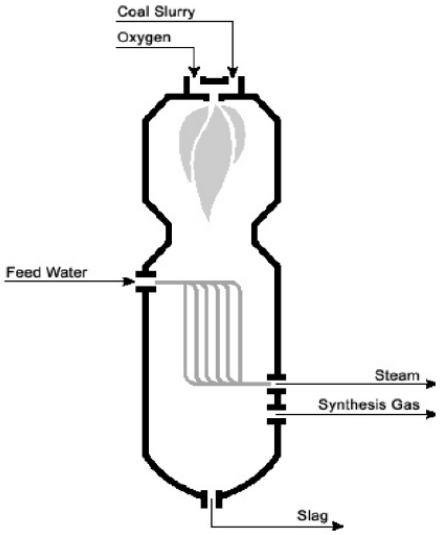

Figure 7 – Illustration of entrained-flow gasifier [29].

In Bubbling Fluidized Bed (BFB) gasifier, the gasifying agent is introduced from the bottom of the equipment and exits from the top as shown in the Figure 8. This reactor is formed of a bed of intergranular materials. Due to the high mass and heat transfer rates, the temperature remains controlled during operation, generally around $650 - 950$℃. Furthermore, the pressure can be varied between 1 and $35\ bar$. A cyclone is used to partition ash and particles from the produced gas, which contains an almost non-existent amount of tar and high amounts of particles [15] [17].

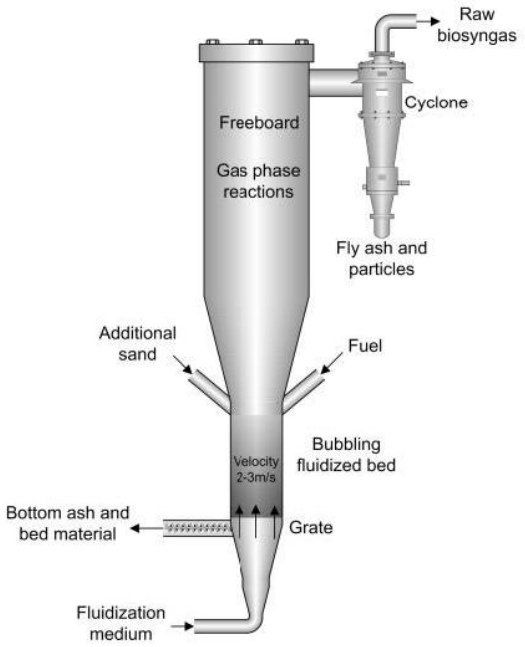

Figure 8 – Illustration of bubbling fluidized bed gasifier (BFB) [29].

Circulating Fluidized Bed (CFB) gasifiers are made of two different units: one unit is the gasifier unit and the other is a circulation unit, as shown in Figure 9 [15]. The operating temperature in this equipment is usually in the range of $800 - 1000$ ℃ and operating pressure can be between 1 and $20\ bar$. In this reactor the ash and hot gas are partitioned by cyclone separator, and the particles are re-circulated to the gasifier. This equipment is considered as a fuel flexible technique, and the producer gas can have a higher quality than the bubbling fluidized bed gasifier, depending on the operating conditions [29].

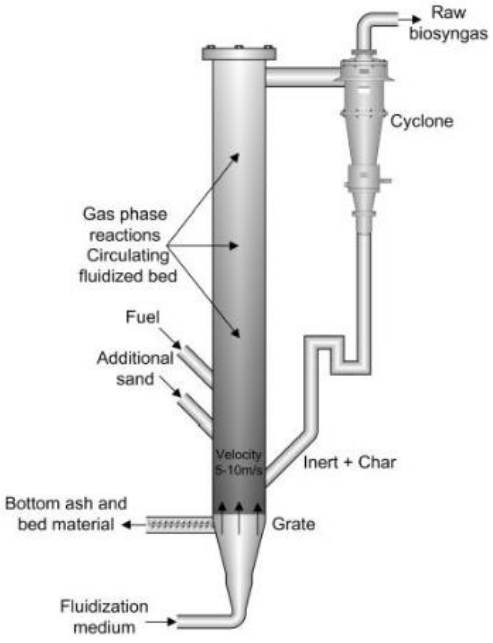

Figure 9 – Illustration of circulating fluidized bed gasifier (CFB) [29].

2.7 Tar Cracker

Tar cracking is the process of converting the tar from the biomass to lighter hydrocarbons. It comprises generally of two routes, thermal or catalytic, which can take place in situ, i.e. inside a gasifier, or ex situ through a reactor. The thermal cracking process generally develops around $1200\,℃$, but the temperature at which this occurs is mostly dependent on the composition of the tar [22]. To obtain adequately high tar cracking high temperature and long residence time are required [30].

The other route to achieve tar cracking is the catalytic cracking, this by passing the raw gas over a catalyst to break down the tar molecules [22]. In this method, an increase in high value products is observed due to the process conditions being less severe than the thermal cracking [31]. The energy consumption of catalytic tar cracking is much less than the thermal route and thus is the preferred option for ex-situ treatment of the tar. Some measure of thermal cracking occurs inside the catalytic reactor, but due to the relatively low temperatures, the tar mostly breaks down due to the reaction.

The choice of catalyst and process conditions determine the conversion and the selectivity of the reactor towards a certain compound. As such, a wide range of products can be achieved by a tar cracking reactor, syngas and light aromatics amongst them. High conversion, especially to BTX, would generally require high pressures [27]. A portion of the feed to the reactor converts into coke, carbon compounds depositing on the catalyst, indicating a loss of products, as well as active sites on the catalysts [32].

2.8 Absorption

Physical removal of tar can be accomplished by using an absorption unit. For the separation to succeed, the tar must condense. In contact with the absorbent, the tar will form droplets that can be separated from the gas phase and then be dissolved in the liquid phase. After the separation, the tar-containing absorbent may be regenerated, combusted or recirculated to the gasifier [33].

The choice of absorbent depends on various factors such as composition of the gas stream, properties, stability and its price. High quantity or cost of the absorbent would indicate a need for recovery. The absorbate will also affect this choice. For example, the solubility of the desired component is important as it influences the amount of absorbent required. Physical properties of the absorbent, such as viscosity, are of importance, as high values would result in lower rates of mass transfer [34].

Vegetable oil has proven to be an efficient absorbent for tar removal in gasification processes. Because of its molecular properties, containing a polar head and a non-polar tail, it is possible to absorb both hydrophilic and hydrophobic tar compounds. Hence, improving the overall efficiency of the absorption process. Experiments, using canola and palm oil conducted by S. Unyaphan et al. showed a removal efficiency up to 97% and complete removal of phenol and naphthalene [35].

2.9 Adsorption by activated carbon

The adsorption method is used in a wide range of industrial applications, including gas and air cleaning from volatile organic compounds (VOC). Activated carbon (AC) is a widely used adsorbent and is made of amorphous carbonaceous raw materials, such as wood, coal, peat or coconut shells. The material could be activated by heating the particles up to almost $1000\,℃$, at which volatile components are removed from the carbon present in the raw material. The pore structure determines the adsorption capacity and properties of the activated carbon [36]. The selection of the most suitable type of activated carbon for a specific application depends on the physical and chemical properties of the substances to be adsorbed [37].

Primarily, adsorption is a physical process, through which the gas is brought into contact with the adsorbent, for example, activated carbon. The substances adsorbed do not undergo any chemical reaction with the adsorbent. VOC molecules are adsorbed on the surface and bound by physical Van-

der-Waals forces with the activated carbon pores. Due to capillary condensation the adsorbed vapor accumulates in the pores of the activated carbon. Thus, VOC bonds with the activated carbon via adsorption until saturation, and the cleaned gas comes out. The saturation level is normally expressed in $g\ adsorbed\ gas/kg\ activated\ carbon$ [38].

Adsorption isotherms can be derived depending on the concentration of adsorbate substance and temperature. This material-specific balance can be calculated for gas phases using empirical isothermic equations such as Langmuir, Freundlich or Radke-Prausnitz for monocomponent and multicomponent adsorbants systems, to estimate the quantity of adsorbate in the adsorbent in mg/g [39]. For higher partial pressures, the adsorption capacity increases, and the activated carbon will have a higher adsorption capacity at high input concentrations at a certain temperature. The capacity, however, decreases with higher temperatures [36].

Adsorption is a reversible process, the reverse process being desorption. When the activated carbon saturation level has been reached, the adsorption capacity falls, and the activated carbon should be replaced by new activated carbon or be regenerated. Regeneration is a sustainable method since the same adsorbent can be used for many cycles. Regeneration can be done through different methods including but not limited to thermal, steam, pressure-swing and chemical regeneration. Moreover, it is possible to combine these regeneration methods to perform for example a thermo-chemical or electro-chemical regeneration. Different parameters should be considered for the choice of regeneration method, such as highest possible degree of desorption of the adsorbate, erosion and mechanical destruction of used adsorbent, as well as easiest separation of recovered compounds from desorbate and the purity of the desorbed components [40].

2.10 Combined heat and power

The simultaneous production of electricity and generation of heat from a single source of fuel is known as cogeneration or combined heat in power (CHP). CHP technologies can use a wide variety of fuels and have been applied for institutional, industrial and large commercial purposes. The fuels that can be used include fossil and renewable options such as coal, natural gas, propane, synthesis gas, biogas, or biomass. CHP systems improve energy efficiency by making use of energy that in other cases is wasted. There are three main different working principles that are commonly used in CHP processes. These principles include the use of steam cycles, air cycles, or combined cycles [41].

2.10.1 Steam cycle

Steam cycles follow four basic steps. First, water is pumped into a boiler at high pressure, coming out of the boiler as supersaturated steam. The high-pressure steam is expanded in a steam turbine where its pressure is reduced, and its energy is converted to mechanical power that is used for electricity generation. The low-pressure steam is then condensed, and the recovered energy is used for district heating. In the final step, the liquid is pumped back to the boiler in order to repeat the cycle. A diagram of the process is shown in Figure 10 [42].

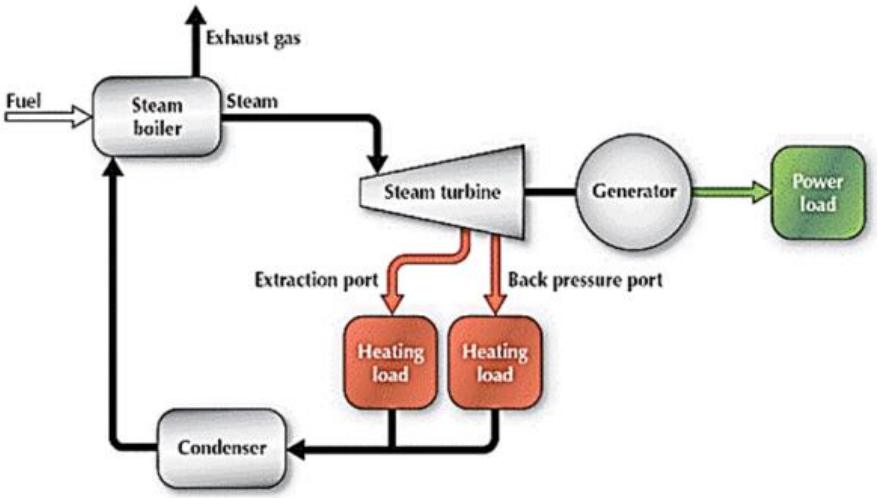

Figure 10 – Steam cycle schematic [43].

2.10.2 Air cycle

Systems that use air cycles include a compressor, a combustor, a gas turbine, and a heat recovery unit. In the first step, the compressor sends pressurized air to the combustion chamber where air is mixed with fuel and heated by combustion to complete the second step. In the third step, the hot compressed air is expanded in the turbine where mechanical work is converted into electricity. One additional step is included in CHP plants that consists of recovering heat from the expanded air stream. This process is illustrated in Figure 11 [43].

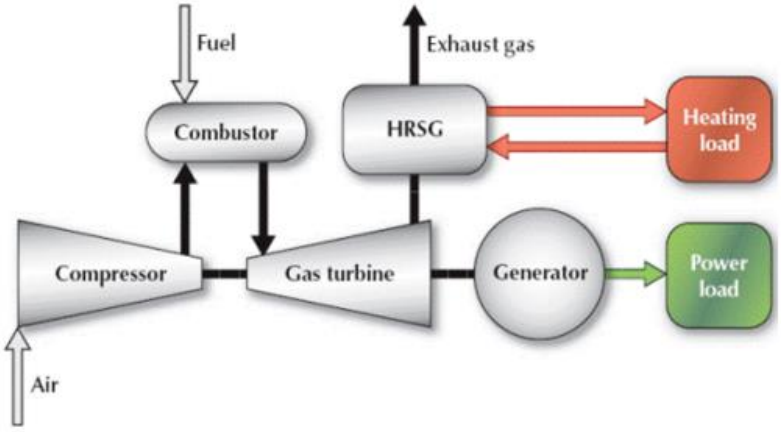

Figure 11 – Air cycle schematic [43].

2.10.3 Combined cycles

A combined cycle includes the two systems described in the previous sections in one single plant. The first part of the process follows the principles of an air cycle, that is, air is compressed, heated by combustion, and expanded in a turbine. However, instead of a heat recovery unit, the expanded gas is used to combust fuel in a boiler, where steam is generated, and the steam cycle starts. This kind of cycles have 2 turbines that can be used for power production and two points where heat can be recovered. A schematic of the process is shown in Figure 12 [43].

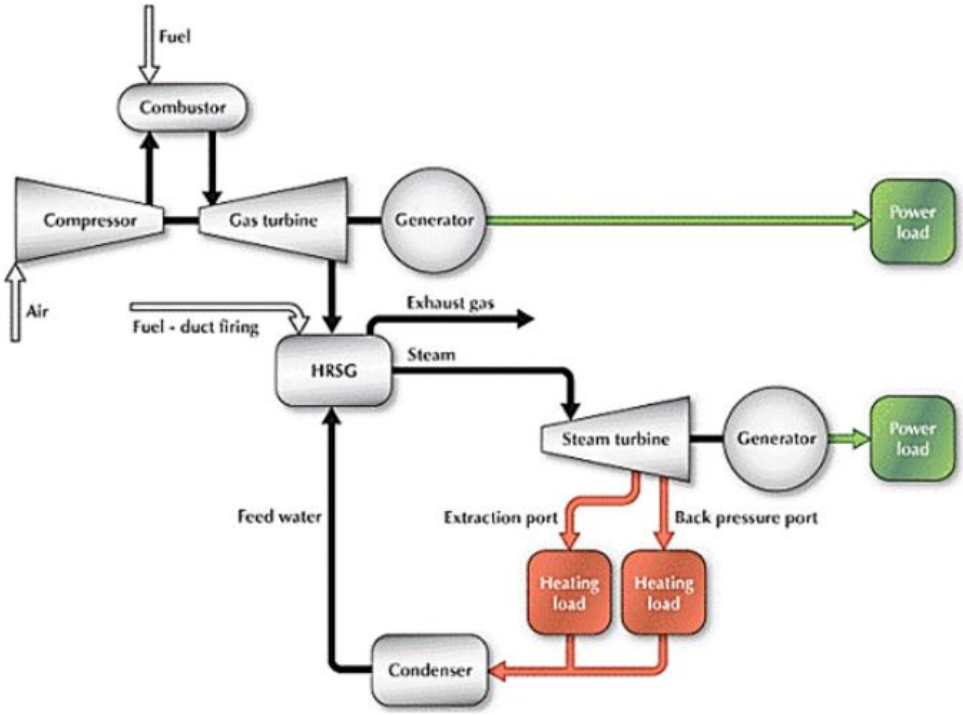

Figure 12 – Combined cycle schematic [43].

3 Process design

The overall process schematic is viewed in Figure 13, while the description for some of the important streams are presented in Table 5.

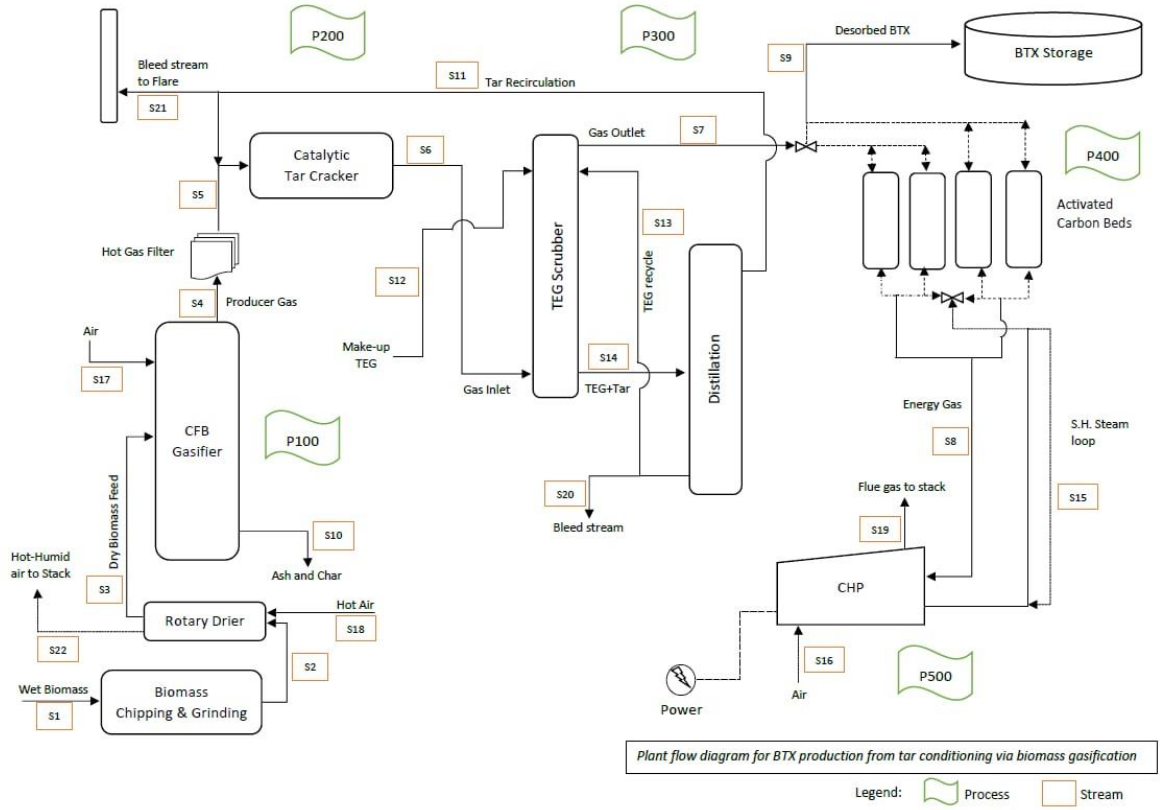

Figure 13 – Proposed process flow sheet for BTX production

Table 5 – Description of streams

Stream	Description
S1	Wet biomass feed to drier $(13.3\ wt\%\ moisture\ content)$
S3	Dried biomass feed to CFB gasifier $(8\ wt\%\ moisture\ content)$
S4	Producer gas (tars, particulates, non-condensable gases)
S5	Producer gas (tar, non-condensable gases)
S6	Producer gas (tar, BTX, non-condensable gases)
S7	Cleaned producer gas (BTX, non-condensable gases)
S8	Energy gas to CHP plant (non-condensable gases)
S9	BTX after desorption from activated carbon bed
S10	Ash and bio-char bottoms
S11	Tar recirculation stream to tar cracker
S17	Air inlet to CFB gasifier
S18	Hot-air inlet to rotary biomass drier
S19	Flue gas to stack
S22	Hot-humid air to stack

3.1 Biomass

Wood chips from Värnamo, Sweden, were used as the fuel source for the gasifier. The data for this was extracted from Phyllis2, and can be viewed in Table 6 [44].

Table 6 – The composition of biomass [44].

Proximate Analysis	As Received ($wt\%$)	Dry ($wt\%$)	Dry and Ash-Free ($wt\%$)
Moisture content	13.3	-	-
Ash content	1.56	1.8	-
Volatile matter	65.46	75.5	76.88
Fixed carbon	19.68	22.7	23.12
Ultimate Analysis			
Carbon	44.56	51.4	52.34
Hydrogen	5.2	6	6.11
Nitrogen	0.26	0.3	0.31
Sulphur	0.03	0.03	0.03
Oxygen	35.09	40.47	41.21
Total	100	100	100
Calorific Data			
HHV (MJ/kg)	17.81	20.54	20.92

In the cases where the above data was not enough, for example with the specific heat, the biomass was correlated with that of black pine [45]. This assumption holds valid due to the fact that 39% of the forests in Sweden comprises of pine [46]. As such, the specific heat was approximated to be $1.341\ kJ/kg.K$.

3.2 Pre-treatment

Raw biomass, preferably forest residues (GROT) or other wood species, are used as the fuel source for the gasifier. The higher moisture content and the irregular sizing of the procured biomass necessitates the use of a drying and particle size reduction/homogenizing equipment, respectively. As a result, the major unit processes employed in this stage were divided into size reduction and drying.

The circulating fluidized bed gasifier was reported to demand a moisture content of roughly $15\ wt\%$ [47], though for this case study, a moisture content of $8\ wt\%$ after drying was chosen, in an attempt to replicate the study by C.M. Kinoshita et al. [48]. Hence, a drier is employed downstream.

3.2.1 Size-reduction of biomass

Details			VHZ 1600
Infeed opening (W × L)		mm	1605x1605
Rotor dimensions		mm	d=430; L=1595
Rotor speed		rpm	90 – 265
Number of counter knives		pcs.	4
Number of cutters	simple	pcs.	37
	double		74
	triple		111
Motor power (frequency converter)		kW	55, 75, 90 kW (75, 90,160 kW)
Total weight (without feed hopper)		t	6,3
Screen hole size		mm	customer-specific
Dimensions (W × H × L)		mm	2250x1580x3360

Figure 14 – Specifications of biomass shredder [49].

The preferred particle size of biomass at the gasifier inlet was fixed to be less than $3\ cm$ [50]. Taking this as the benchmark, biomass shredding and drying was modelled. However, it was noted that the biomass undergoes a shrinkage during the drying stage when the bound moisture leaves the fibers. As a result, the outlet particle size is fixed to $3.5\ cm$ accounting to the 26% shrinkage for pine wood [46]. As seen from Figure 14, the received biomass passes through the shredder where the larger chunk of material is broken down into a predefined size. This quantity of material then moves on to the rotary drier for moisture reduction. The specifications for the stream are found in Table 7.

Table 7 –Stream data for biomass entering the drier.

Characteristics of stream (S1=S2)	Parameter values
Flow of wet biomass (13.3 wt% moisture)	$2.81\ kg/s$
Temperature	$25\ ℃$
Pressure	$1\ bar$

3.2.2 Biomass Drier

The drying process is carried out in an air-blown directly-heated single-pass rotary drier. Even though driers can be operated with superheated steam, this possibility was ruled-out since the gasifier was optimized for tar production with air as input. This implied that the superheated steam at the outlet of drier cannot be directed into the gasifier and letting it out to the atmosphere meant a loss in energy efficiency. Therefore, a rotary drier with co-current flow of heated air and wet-biomass was chosen, as illustrated in Figure 15.

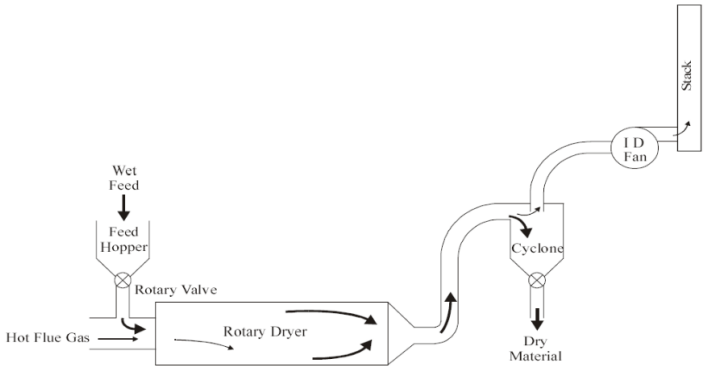

Figure 15 – Depiction of a single-pass rotary drier [10]. Hot air is used instead of hot flue gas.

The aim of this process is to reduce the moisture content from $13.3\ wt\%$ [44] to $8\ wt\%$ [48]. The inlet temperature of heated air to the rotary drier was set at 230 ℃. Also, a co-current flow of hot-air and biomass feed was considered, so that the wettest part of biomass came into contact with the hot inlet gas [10]. Table 8 shows some parameters of importance for the drier, calculated based on formulae extracted from [51] [52]. The mass and energy balances are provided in Section 4.1.

Table 8 – Operating conditions for biomass drier

Operating Conditions	Value
Drier	Rotary, single-pass
Type	Air-blown, co-current flow
Residence time	$11.45\ seconds$
Heat required to evaporate moisture (Q_1)	$0.29\ MW$
Heat required to increase temperature of wood chips (Q_2)	$1.09\ MW$
Heat required to increase temperature of air (Q_3)	$0.15\ MW$
Total heat energy needed $(Q = Q_1 + Q_2 + Q_3)$	$1.53\ MW$

3.3 Gasification

As mentioned, the product from gasification is dependent on type of gasifier and the operational conditions. For a capacity of $50\ MW$ of biomass, some possible gasifier technologies are entrained-flow, BFB and CFB gasifiers, as fixed bed gasifiers are only applicable for capacities below $10\ MW_{thermal}$. As entrained-flow gasifiers are designed to produce virtually no tar, i.e. no BTX, they were not considered further in this study [19].

In comparing CFB and BFB, H. Karatas et al. reported that the BFB has lower agglomeration and corrosion potentials [53], but on the other hand, P. Mitsakis reported that CFB not only yields more tar, but the tar also contains a higher fraction of BTX [54]. For this reason, CFB was chosen as the suitable gasifier.

As tar is typically an unwanted side product, most recent research regarding gasifier parameters focus on minimizing tar production. As the aim of this study was to produce BTX, and BTX typically makes up a large portion of the tar, the gasifier should in theory be run to maximize the tar production. An important factor for this is the gasifying agent, which typically is steam, air or a mixture of oxygen and steam. While steam and/or a mixture of steam and oxygen have been reported to give high tar contents, injection of steam introduces other complications such as higher steam content in the producer gas and a need for optimization of the ratio between steam and oxygen supply [55]. Thus, for simplicity, only dry air was considered in this study.

Equivalence ratio (ER) is a key parameter when using air, and it is defined as

$$ER = \frac{Oxygen\ supplied}{Stoichiometric\ oxygen\ amount} \quad (9)$$

Where the stoichiometric oxygen is the amount of oxygen required for complete combustion of the biomass. The oxygen will allow combustion reactions to occur to some extent, supplying heat to the system, and should be in the range of $0.2 - 0.4$ for effective gasification [56].

Naturally, temperature and residence time are also important parameters. Higher temperatures have been reported to reduce tar content, and this is connected to ER since the combustion reactions are exothermal. Higher temperatures and longer residence times allow more tar to be cracked [56], thus, the temperature should not be too high and the residence time relatively low.

C.M. Kinoshita reported a maximum in tar yield as well as benzene fraction at 750 ℃ [48], and this temperature was chosen for the CFB in this study. Following the more detailed study by J. Gil et al., a maximum in tar yield using air as gasifying agent was reported for an ER of roughly 0.25. Table 9 below shows the corresponding gas composition, LHV and tar yield applied in this study. Important to note is that this data is from a BFB gasifier, as no detailed data for high tar production was found for CFB gasifiers.

A hot gas filter was as well placed after the gasifier to remove dust and particles in the producer gas, in order to protect the downstream equipment, e.g. the heat exchanger, the tar cracker catalyst and the scrubber. In addition, the efficiency the downstream equipment might increase in the absence of particles and dust. The fact that the filter withstands high temperature, helps in avoiding unwanted condensation of moisture in producer gas [57].

Table 9 – Dry gas composition from the gasifier, LHV and tar yield at ER = 0.25 [55]

Component	**H_2**	**CO**	**CO_2**	**CH_4**	**C_2H_n**	**N_2**
Fraction $(mol\%)$	11	19	14	4.8	2.5	48.7
Tar yield $(g/Nm^3\ dry\ gas)$	30	LHV $(MJ/Nm^3\ dry\ gas)$				6.1

3.4 Tar cracker

3.4.1 Catalyst

The ideal catalyst for this process should have high activity and efficiency of tar conversion in a temperature range of $500 - 900$ ℃, with high concentrations of H_2, CO, CO_2 and H_2O. Moreover, it has to be resistant to coking, poisoning, sintering and attrition, as well as be easy to regenerate and have environmental suitability. An important factor in the choice of catalyst is its economic and commercial availability [58]. Furthermore, the catalyst of choice, for the purpose of this project, should be selective to the formation of either one or all of the BTX components, while satisfying conditions such as low pressure and high conversion.

The catalyst can be chosen from a wide range of options. Natural minerals such as dolomite, olivine, calcite or magnesite, or synthetic heterogeneous catalysts such as zeolites, carbon-supported catalysts, metal-promoted zeolites, transition metals, noble and alkali catalysts have all been investigated [58]. Dolomite and olivine are the most commonly used minerals for this purpose, and both have the advantage of being cheaper than the synthetic catalysts and being naturally available, hence requiring comparatively less treatment. Experiments conducted by Boot-Handford et al. has shown that the dolomite converts $98\ wt\%$ of the biomass tar at 900 ℃ [59], and according to Henrik Aldén et al. calcined dolomite converts naphthalene to BTX with a 96% conversion at 800 ℃ [60]. However, this catalyst is more fragile than the olivine catalyst, and both catalysts as well as the rest of the natural catalysts show lower catalytic activities and have a shorter lifetime quicker than synthetic catalysts [58].

Among the synthetic catalysts, the carbon-supported catalyst is less expensive than the other types. It occurs naturally in the gasifier, in the form of char, but is rapidly deactivated due to coke formation. Alkali metal and noble-metal-based catalysts have high catalytic activities, but on the other hand the alkali metal catalysts could evaporate easily. Noble-metal-based catalysts are more advantageous because of their long stability and high carbon deposition resistance [58].

Another type of synthetic catalysts are the transition metal catalysts such as Ni, Fe and Ca, which presents a high catalytic activity but have the disadvantage of being deactivated by carbon deposition on the catalyst surface [58].

Zeolites catalysts have high thermal/hydrothermal stability, high resistance to sulfur and the possibility to be regenerated, but they could be deactivated due to the coke formation. The HZSM-5 zeolite converts the biomass tar to BTX at 400 ℃ and atmospheric pressure with a $92.9\ mol\%$ of selectivity and $25.1\ wt\%$ of yield [58].

Most of the catalysts that crack the tar into the desired products, benzene, toluene or xylene, require relatively high pressures of between $1 - 3\ MPa$ [58] and despite the high conversion shown by some of those, they could not be used. As such, a zeolite fluid catalytic cracking (FCC) catalyst was chosen for the tar cracking process, able to work at a temperature of 450 ℃ and pressure of $1\ bar$, with high selectivity towards benzene, albeit a relatively low conversion of tar [27].

The FCC catalyst is commercially available in fresh and equilibrium forms, known as Cat-F and Cat-E, respectively, designed for the purpose of converting the alkyl-aromatic, naphthenic-aromatic, and polyaromatic hydrocarbons. Details regarding both catalysts can be viewed in Table 10 [27].

Table 10 – Properties of FCC Catalysts Cat-F and Cat-E [27].

	zeolite					specific surface area ($m^2\ g^{-1}$)			acidity (μmol of Py g^{-1})					
									Brönsted (1545 cm^{-1})			Lewis (1450–1460 cm^{-1})		
catalyst	UCS (nm)	load (wt %)	Si/Al	RE content (wt %)	metals (Ni + V) content (wt %)	matrix	total	average mesopore diameter (nm)	150 °C	300 °C	400 °C	150 °C	300 °C	400 °C
Cat-F	2.456	22.00	3.5	0.94	0.000	92	243	8.45	128.5	102.1	76.3	118.1	42.4	36.9
Cat-E	2.430	9.83	14.2	0.70	0.095	102	162	8.92	5.0	5.1	5.0	13.6	11.0	10.9

According to the experiments conducted by Richard Pujro et al., Cat-F provides a higher conversion than the Cat-E for the biomass tar. This occurs due to the Cat-F having more acidic sites and crystalline structure. As seen in Table 11 however, the selectivity of Cat -E towards benzene is higher and thus, it is more suitable of the two options [27].

Table 11 – Selectivity of benzene and coke (%) with the catalysts Cat-F and Cat-E [27].

	Cat-F				Cat-E			
	benzene		coke		benzene		coke	
reaction time (s)	2	6	2	6	2	6	2	6
1PhO	51.94	36.46	21.59	26.33	74.64	63.29	9.59	14.04
biphenyl	64.93	55.75	32.56	42.21	82.02	67.43	14.66	28.59
fluorene	78.75	79.52	7.24	11.53	89.48	87.27	2.50	4.61
9,10DHP	12.27	14.38	9.45	15.10	14.77	11.69	2.00	4.08
naphthalene	60.68	51.02	35.11	41.29	87.86	83.43	8.58	14.53
phenanthrene	66.37	49.75	25.14	44.65	76.11	60.10	15.91	32.01
pyrene	96.74	93.50	2.62	5.66	92.55	75.32	5.73	20.93
BaA	80.04	67.76	16.87	29.18	89.35	80.49	8.05	17.51

Moreover, the data from Table 11 indicates that longer reaction times would result in an increase in coke yield and a decrease in benzene yield. On the other hand, a higher conversion can be achieved

with longer residence times, as seen in Figure 16. In this case, using Cat-E with a residence time of 2 $seconds$ yielded the highest amount of benzene.

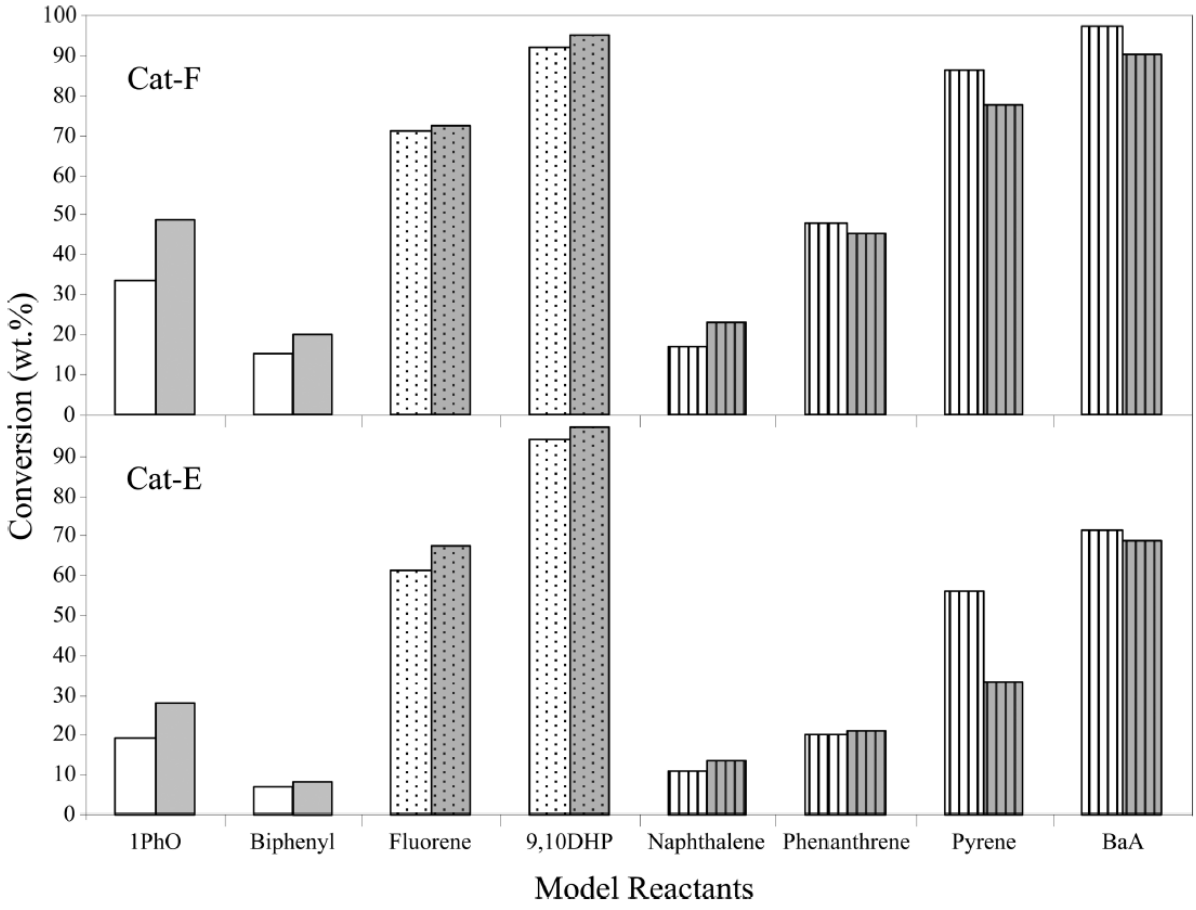

Figure 16 – Conversion of the tar model reactants for Cat-E and Cat-F. White: 2s residence time, grey: 6 s residence time [27]

3.4.2 Catalytic reactor

Fluid Catalytic Cracking (FCC) is one of the most important and developed technologies in the refinery industry [61]. As can be seen in Figure 17, the process consists of a cracking reactor and a catalyst regenerator providing continuous regeneration of the catalyst while converting the tar at the same time [62]. In the conventional FCC process, the catalyst particles, steam and the gas come into contact in the riser, which could serve to evaporate the oil gas stream, in case of it being in liquid phase, as well as causing the upward movement of the gas and catalyst, with the reaction proceeding along the length of the reactor. Temperature drop might occur due to evaporation and the endothermic reactions. Furthermore, the reactions produce large quantities of coke, hence there is need for a regeneration unit, to which the catalyst can be introduced in order to eliminate the coke by burning it with air and which can then be recycled back into the reactor. The regenerator also provides the benefit of energy production, from coke combustion, which is used in the reactor, making the process more efficient [62] [61].

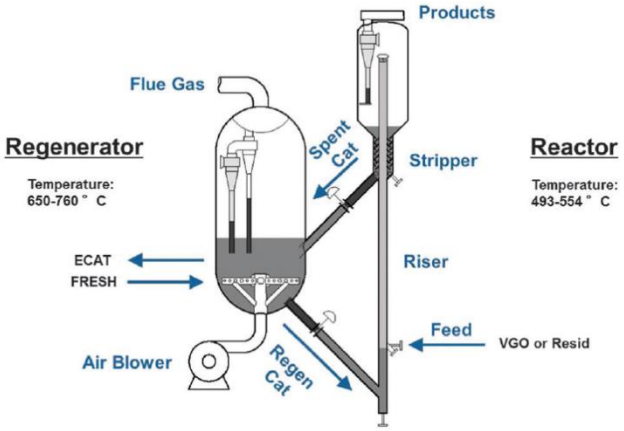

Figure 17 – Fluid catalytic cracking process (FCC) [61].

3.5 Absorption and regeneration

The OLGA technology (oil-gas scrubber), developed by the Energy Research Center in the Netherlands and Royal Dahlman, is a tar removal process for the cleaning of producer gas from biomass gasification using an oil. The process consists of various steps including condensation, absorption, stripping, separation and regeneration. A schematic diagram of the process is shown in Figure 18. In the first step, heavy tars will be removed by condensation, while in the second part light tars will be removed through absorption. Hence, the scrubbing oil does not come in direct contact with the tars. The oil can be regenerated and both heavy and light tars can be directed back into the gasifier for its destruction [63]. The advantage of the OLGA process is the ability to regenerate the scrubber oil, which in turn decreases the operating cost for the plant.

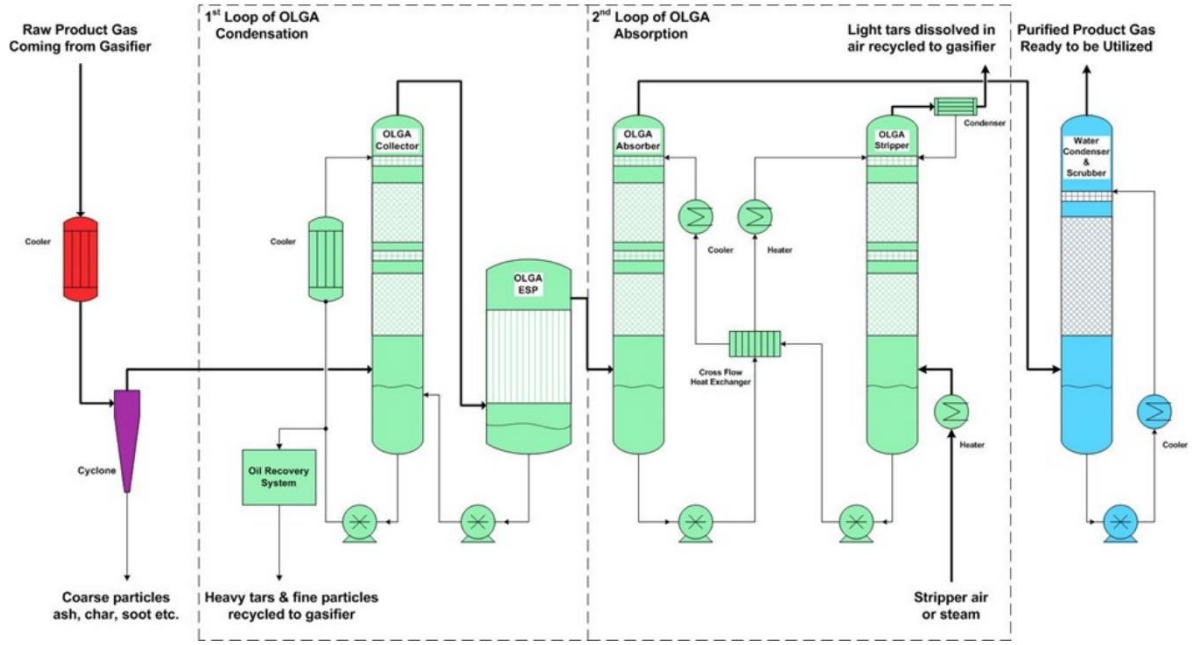

Figure 18 – Schematic diagram of the OLGA process

Gothenburg Biomass Gasification (GoBiGas) was a project designed to demonstrate production of biomethane using gasification on a commercial scale. The project started in 2005 and had a production of $20\ MW$ biomethane. Tar removal was performed by cooling of the producer gas prior to particle filtration. Afterwards the gas was cleaned in a scrubber using rapeseed-methyl-ester (RME). Estimated values of tar in the product gas after scrubbing were 0.034% naphthalene and 0.001% other tar

compounds and the input of RME was approximately $3.3\ MW_{RME}$ per $100\ MW_{Biomass,DAF}$. The saturated RME would be fed into a combustor for heat recovery [64].

Tar removal by absorption can also be performed using waste cooking oil. A study investigating the performance of waste cooking oil compared to vegetable oil was conducted by Paethanom et al. showing a removal efficiency of 63.6% for vegetable oil (mixture of canola and soy-bean oil) and 56.4% for waste cooking oil. The lower performance of waste cooking oil was assumed to be because of the smaller surface area caused by contaminants from previous usage of the oil. Furthermore, it was shown that by agitation and thereby decreasing bubble size, the tar removal efficiency could be increased by approximately 25% for both types of oil [65].

Problems with absorption in gasification plants include the production of waste streams. The possibility to regenerate the absorbent can lead to a more economically viable process and also a more sustainable process in the sense of reducing the amount of waste produced. The possible technologies for absorbent regeneration are stripping columns, as used in the OLGA process and a less energy intensive process, centrifugation. Other alternatives to be considered are crystallization, distillation or liquid-liquid extraction. However, for centrifugation it is only possible to remove insoluble tars [66], meaning that even if the absorbent is regenerated to some extent there will be accumulation of tars in the liquid and the absorbent must be replaced after some time.

Fractional distillation of coal tar is an industrial process to retrieve valuable components of tar such as naphthalene, pitch, pyridine and benzol [67]. Considering the possibility to extract fractions of tar by distillation makes it a promising technique for regeneration of the absorbent.

In this project, absorption was used as the main process for separating tar from the gas-phase. The separated tars were recycled back into the tar-cracker and the absorbent is sent to a regenerator. The choice of this unit was highly dependent on the type of absorbent used. previously. The units were simulated using Aspen Hysys V10 and the conclusions were based on the results from that.

As RME (i.e. methyl oleate) had the same boiling point as tar (here approximated as naphthalene), a distillation column was not suitable. It has already been shown in the OLGA process that regeneration of RME is a possibility, however, data regarding OLGA was not accessible as it is a patented process. As such, liquid-liquid extraction (LLE) was tried for this. The aim of LLE was to find an organic solvent, able to extract high amounts of naphthalene, yet volatile enough, so that it could be evaporated afterwards, hence achieving separation of the solvent, RME and tar, so that they all could be recycled back to their respective processes. LLE has been a method of BTX-extraction in the naphtha cracking process, so most of the solvents tried for this project were the ones used for LLE in classical BTX-production methods, such as diethylene glycol, sulfolane or dimethyl sulfoxide [68]. Other common solvents were also tested with the software; ethers, methanol, ethanol, hexane and cyclo-hexane being amongst them. None of the solvents were able to perform in the LLE unit though, but some showed ability to be used in the absorption column instead of RME, for example, sulfolane, dimethyl sulfoxide, diethylene glycol (DEG) and triethylene glycol (TEG).

Ethers, methanol, sulfolane and dimethyl sulfoxide were not as good absorbents as RME, some also evaporating inside the column, and thus had to be disregarded. Glycerol, while not showing such behavior, suffered from low absorption, but could be regenerated by distillation. DEG was quite adequate in tar removal, but TEG showed the best removal amongst all the tested absorbents other than RME. The boiling point difference between naphthalene and TEG was also high enough to allow for distillation and achieve almost pure components for recirculation.

One main problem, as is explained in more detail in section 4.4.1, was the presence of water in the inlet gas to the absorber, and uncertainty on its effects on the absorption process. Due to time

constraints in the project and a relatively low fraction of water in the gas, the effect of the water was ultimately neglected, and it was assumed to simply leave the absorption column with the gas. In case that this was not true, a dehydration unit would be required before the absorption column. Dehydration of natural gas is a widely investigated process and following a similar route can also be recommended here. Three options are available for this [69]:

- Adsorption, with silica gel and alumina being the most common adsorbents [69]. Axsorb Activated Alumina especially shows good potential for dehydration purposes [70].
- Condensation, dependent on the dew point, and would result in losses in tar and BTX most of all, because they would also condense with water, meaning another separation method would also be required to recover the condensed products. Formation of hydrates could also be problematic in this case [69].
- Absorption, for which TEG itself is the best dehydrating means. A reboiler at high temperature will also be required to boil the water out of TEG and reuse the purified TEG [69].

3.6 Activated carbon adsorption

After the absorption process, a mixture of energy gas, BTX and water vapor remain. Different methods could be used to extract BTX from the mixture, some options being absorption, adsorption, condensation, or thermal and catalytic oxidation. The adsorption process in porous materials such as activated carbon was chosen as it is considered the most selective for BTX adsorption and that the activated carbon is an adsorbent with high removal efficiency, low cost, as well as being a regenerable material [71]. Moreover, activated carbon has a large surface area within the range of $700-1500\ m^2/g$. This internal surface is mainly hydrophobic and ideal for the adsorption of volatile organic compounds such as BTX [36].

According to Donau Carbon GmbH, a German supplier of activated carbon, the air cleaning applications require activated carbon grades with excellent hardness characteristics combined with high retentivity. Thus, coconut shell based activated carbons (Desorex and Oxorbon) with high hardness and large micropore volumes are the best choice for this field of application. Therefore, Desorex K43 was proposed by the company as the most suitable for the removal of hydrocarbons including BTX [72]. Desorex K43 becomes saturated with $340\ g\ benzene\ /\ kg\ activated\ carbon$ at 20 ℃ and the $partial\ pressure/saturation\ pressure\ (p/p^*)$ is 0.1 [72].

The adsorption process is exothermal, which means energy is released into the bed. The optimum temperature for the adsorption is in the range of $15-80$ ℃ and a relative humidity $< 70\%$. Moreover, the adsorption efficiency depends on the type of pollutant and activated carbon used and the temperature and humidity of the waste gases, but the expected yield is between $95-98\%$ VOC removal [36]. For this project, the optimum temperature for full adsorption of BTX on Desorex K43 was found to be around 20 ℃, however, according to Aspen Hysys a stream with a temperature of at least 55℃ was necessary in order to avoid the formation of a liquid phase in the bed.

The desorption process is endothermal, thus energy has to be added to desorb the BTX and regenerate the activated carbon. The regeneration can be denoted as a combination of desorption and activation of the adsorbent. As the activated carbon is regenerated and re-used, material consumption is reduced as less activated carbon is consumed over time [37].

Since hydrophobic adsorbates such as BTX desorb at temperatures approaching or higher than their boiling points, steam regeneration has proven to be very effective and economic to regenerate activated carbons. Steam is cheap and could be produced by a boiler unit which is available at relatively low cost. In addition, steam works well with hydrophobic organic compounds such as BTX, where the adsorbed BTX desorbs from the activated carbon at temperatures approaching steam

boiling point via condensation [40]. In addition, steam has a high energy efficiency, and the high heat of steam condensation allows the bed to be heated up rapidly, allowing for a faster desorption from the adsorbent, this takes place at temperatures between 80 and 200 ℃ [36].

The condensed adsorbate BTX desorbs from the activated carbon and the activated carbon will be reactivated for the adsorption process. Since BTX compounds are non-polar, they can be separated from water by means of a condenser as shown in Figure 19 [73].

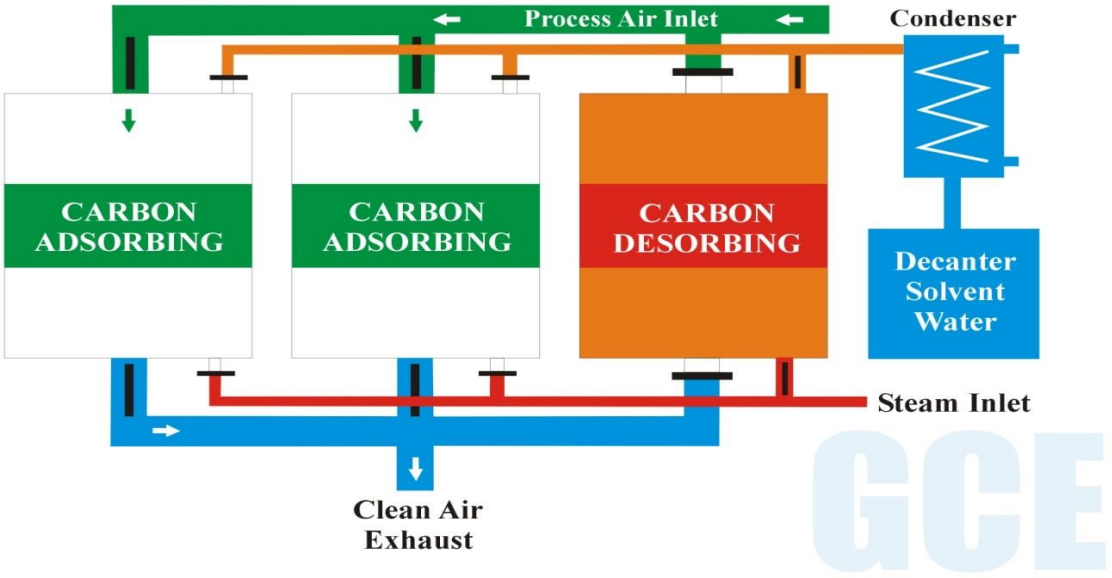

Figure 19 – Steam regeneration of activated carbon [73].

In this project, to regenerate activated carbon and separate BTX at the same time, thermal regeneration by heating up the bed to 200 ℃ was employed, for which the indirect steam jacket is an appropriate approach to desorb most of the BTX from the activated carbon. This temperature is to ensure that no BTX remains adsorbed. After desorption, the bed should be cooled continuously until the desired temperature for the adsorption step is attained in the bed.

The most used activated carbon adsorption beds are fixed beds and fluidized beds. Fixed bed is widely used for air treatment, due to the ability to control the continuous VOC vapor with different flow rates, as well as granting the possibility to regenerate activated carbon sites [73].

3.7 Combined heat and power

As a secondary goal, the project aimed to produce power and district heating. For this purpose, a section for the production of combined heat and power that uses a steam cycle was included in the process. This type of cycle was chosen due to the fact that steam is necessary to increase the temperature in the desorption process to recover BTX from activated carbon. Therefore, the production of steam was considered in the process. The principles explained in section 2.10.1, with the addition of a second turbine, were used for production of heat and power in this project. The reason to add the extra turbine was that some of the steam produced from the boiler is used in the desorption process and the rest of the heat is expanded to generate an extra amount of power. With this modification, the process features the following steps.

- Water is pumped to the boiler
- Supersaturated steam is generated

- Steam is expanded in the first turbine
- Steam is divided into two streams
- A fraction of the steam is used to heat the desorption process
- The rest of the steam is expanded in the second turbine
- Both steam fractions are condensed in separate condensers
- Liquid water obtained from the condensers is pumped back to the boiler to repeat the cycle

A diagram of the process is shown in Figure 20.

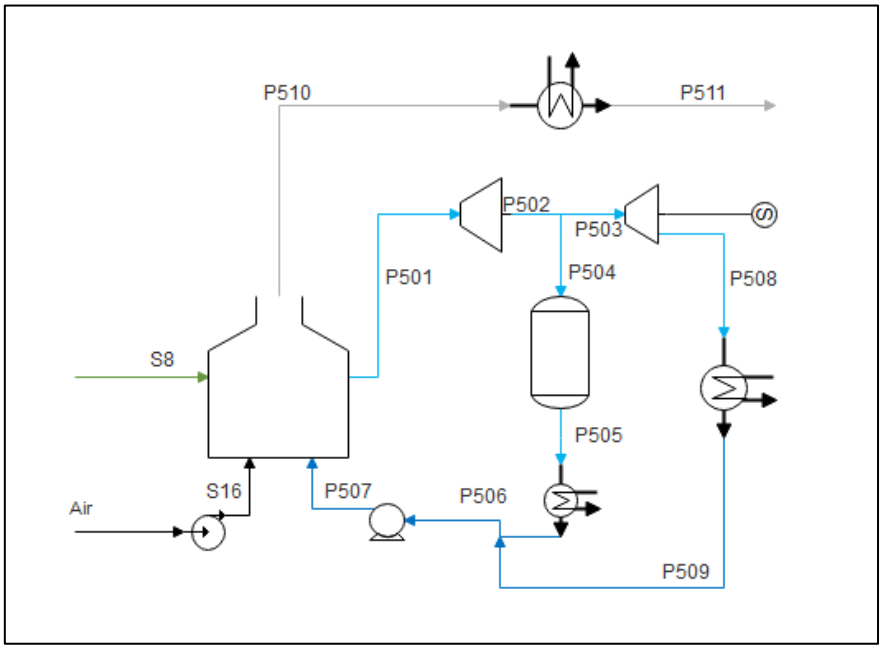

Figure 20 - Combined heat and power process

The energy gas separated from BTX and tar will enter the CHP plant. The gas is composed of hydrogen, carbon monoxide, carbon dioxide, methane, nitrogen, and a small fraction of the benzene, toluene and xylene that was not recovered in the adsorption step. The heat obtained from the combustion of this gas was used to calculate the amount of steam that can be produced. For the mass and energy balance around the boiler, an excess of 120% of air at $25\,℃$ was considered. The mass flow, composition and temperature of the energy gas was known from the previous step. The water entering the boiler was considered to be saturated liquid at the same pressure of the produced steam which was chosen to be at $45\,bar$ based on information about CHP obtained from the U.S. Department of Energy [42]. The temperature of the steam leaving the boiler was calculated based on the temperature of the steam required for desorption of BTX from activated carbon. For the desorption process, supersaturated steam at $200\,℃$ and $3\,bar$ was chosen. This data together with an isentropic efficiency of 85% for the turbine was used to calculate to temperature of the steam before the first turbine and after the second one. The steam leaving the second turbine was considered to be at $1\,bar$ and the steam that leaves the desorption process was considered to be at $140\,℃$ and $3\,bar$. Both steam streams are condensed and leave the respective condensers as saturated liquid. Finally, they are pumped back to the boiler at $45\,bar$ and the cycle is repeated.

A combined cycle was another option that could have been used to generate steam, but it was not considered as they usually require the use of extra amounts of fuel to generate supersaturated steam. Combined cycles and other possibilities such as flue gas condensing were not analyzed in detail due to time limitations.

4 Mass and energy balances

Looking closer at the calculations performed, the process shown in {entire PFD} was divided into the separate unit operations. Mass and energy balances were set up over each unit, and the flows were then scaled up to all be based on the same initial amount of biomass. Some general assumptions applied in the study were

- Ideal gas behaviors
- Isothermal and isobaric processes, excluding the absorber, regenerator and steam cycles
- No pressure drops in between processes, so potential fans and pumps were excluded from the process design
- Specific heat capacities are constant, with the exception of certain tar compounds where the value changes significantly after phase change
- Potential fan and pump work are neglected
- Air is dry and consists of 21 $mol\%$ oxygen and 79 $mol\%$ nitrogen
- No heat losses due to convection other than for the boiler
- No kinetic or transport limitations
- The entire heat exchanger network was not studied, and for most unit processes the heat exchanger medium was not considered

The energy balances were generally performed with a reference state of 25 ℃ and 1 atm, yielding the heat released or required for each process. Table 12 below shows the thermodynamic data applied in the energy balances. Table 13 shows the additional thermodynamic data that was applied to the tar cracker.

Table 12 – Thermodynamic data applied in energy balances [74]

Compound	$\Delta_f H^\circ\ (kJ/mol)$	$C_{p,i}\ (J/mol.K)$	Boiling point (K)	$\Delta_{vap} H^\circ\ (kJ/mol)$
Benzene	49	143.57	354.8	32.9
Toluene	12	157.09	383.8	33
Xylene	−24.4	187.65	410.85	39.45
Naphthalene	77.95	196.06	491	68.6
H_2	0	29	-	-
CO	−110.53	30.8	-	-
CO_2	−393.51	32.51	-	-
CH_4	−74.5	34.82	-	-
N_2	0	29.12	-	-
O_2	0	9.21	-	-

Table 13 – Thermodynamic data for additional tar compounds [74]

Compound	$\Delta_f H^\circ\ (kJ/mol)$	$C_{p,i,s}\ (J/mol.K)$	$C_{p,i,l}\ (J/mol.K)$	$C_{p,i,g}\ (J/mol.K)$
1-PhO	−96.1	-	291	441.87
Biphenyl	100.5	198.39	285.3	-
Fluorene	90.2	203.13	-	189.5
9,10-DHP	66.3	243.08	-	354.45
Phenanthrene	77.95	220	-	334.16
Pyrene	120	228	-	387.64
Benzanthracene	170.8	273.6	-	468

Table 14 – Thermodynamic data for additional tar compounds [74]

Compound	Fusion point (K)	Boiling point (K)	$\Delta_{fus}H^{\circ}$ (kJ/mol)	$\Delta_{vap}H^{\circ}$ (kJ/mol)	$\Delta_{sub}H^{\circ}$ (kJ/mol)
1-PhO	-	532.5	-	66.2	-
Biphenyl	342	528	19	54.2	-
Fluorene	387.9	571.2	-	-	83.9
9,10-DHP	370	441.7	12.8	72.3	-
Phenanthracene	343	609	-	-	90.2
Pyrene	425	651.36	-	-	100
Benzanthracene	432.25	710.75	-	-	110

The following sections shows the solution method and results for each unit process, with detailed calculations listed in the appendix.

The mass flow of the biomass into the process was calculated using the HHV for the chosen biomass provided by Phyllis, as received, viewed in Table 6.

$$F_{S1} = E_{S1}/HHV_{BM,AR} = 50/17.81 = 2.81\ kg/s \quad (10)$$

4.1 Pre-treatment

The entire section of pre-treatment was divided into chipping and grinding of biomass (shredding) and the subsequent drying stage.

4.1.1 Biomass Shredding

There is no specific need for a mass and energy balance for this unit process due to the absence of any chemical conversion or parameter changes. The process only involves a physical change of state and reduction in particle size is achieved.

4.1.2 Drying

Stream properties for the inlet and outlet streams from the gasifier are mentioned in Table 15. More detailed calculations on the drier energy balance are presented in appendix 8.1.

Table 15 - Stream mass and energy balance for rotary air-blown drier

Inlet Stream: Hot-air (S18) (Relative Humidity < 1)		**Outlet Stream**: Hot Humid-air to stack (S22)	
Mass flow rate	$11.7\ kg/s$	Mass flow rate	$11.84\ kg/s$
Temperature	230 ℃	Temperature	103 ℃
Pressure	$1\ bar$	Pressure	$1\ bar$
	$Energy\ provision\ =\ 1.53\ MW$		
Inlet Stream: Biomass feed (S2)		**Outlet Stream**: Dry biomass to gasifier (S3)	
Mass flow rate	$2.81\ kg/s$	Mass flow rate	$2.67\ kg/s$
Temperature	25 ℃	Temperature	230 ℃
Pressure	$1\ bar$	Pressure	$1\ bar$
	$Energy\ consumed\ =\ 1.53\ MW$		

As seen from the mass balance, hot-air stream (S18) dries the biomass feed from $13.3\ wt\%$ to $8\ wt\%$ moisture. The air inlet is not saturated and does not contain significant amount of moisture. The hot-air aids in heating up the biomass, ultimately drying it to the desired moisture content. The flow rate of hot-air that can achieve this case-specific moisture reduction was calculated to be $11.7\ kg/s$. Biomass particles have an estimated residence time of $11.45\ seconds$ inside the drier. At the exit of the rotary drier, the air leaves at a temperature of 103 ℃ to the stack, while the biomass is heated to 230 ℃. An important factor in this model is that, the air outlet temperature is maintained at sufficient

levels to prevent condensation of evaporated water in pipelines leading to stack. Similarly, the temperature of dried biomass leaving the drier, is set at a temperature below its ignition point of 260 °C [10].

4.2 Gasification

Figure 21 shows the system boundary of the gasifier unit. As it was not within the scope of this study to simulate the gasification process, the mass and energy balances over the gasifier was based on the data presented in Table 9. More detailed calculations are shown in the appendix.

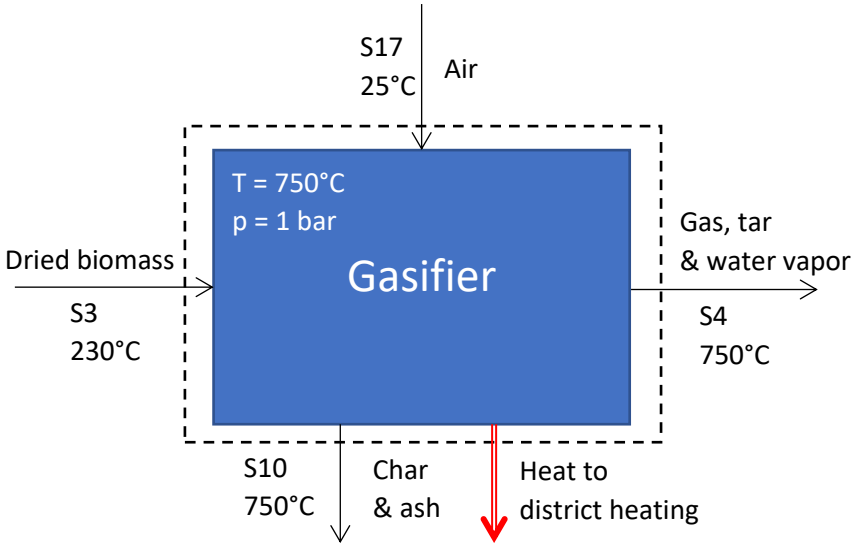

Figure 21 - *System boundary for mass and energy balance over the gasifier*

Some additional assumptions made for the gasifier were

- The nitrogen and sulfur content of the biomass are negligible
- C_2H_n in the gas is negligible
- In the mass balance, tar assumed to consist of the compounds shown in Table 4
- In the energy balance, tar can be approximated as BTX and naphthalene
- Char contains only carbon
- Energy and potential melting of the ash is neglected

The results from the mass balance are summarized in Table 16 and Table 17 and the results from the energy balance are summarized in Table 18 and Table 19.

Table 16 – Summarized results from the mass balance over the gasifier unit

Inlet				**Outlet**	
Component	S3 (kg/h)	Component	S17 (kg/h)	Component	S4 (kg/h)
Carbon	4503	O_2	3167	H_2	172.5
Hydrogen	525.7	N_2	10425	CO	2682
Oxygen	26.67	Total	13593	CO_2	4172
Moisture	763.8			CH_4	602.2
Ash	157.8			N_2	10425
Total	9496			Water vapor	2232

Table 17 – Summarized results from the mass balance over the gasifier unit, continued

Outlet continued			
Component	S4 (kg/h)	Component	S10 (kg/h)
Benzene	233.9	Char	667.9
Toluene	58.47	Ash	157.8
Xylene	29.24	Total	825.7
1-PhO	52.04		
Biphenyl	15.20		
Fluorene	15.20		
9,10-DHP	15.20	Total amount of dry gas (kg/h)	
Naphthalene	52.62	18054	
Phenanthrene	21.05	Total wet gas (kg/h)	
Pyrene	2.339	20286	
BaA	2.339	Total tar (kg/h)	
kg tar per kg dried biomass $(wt\%)$	5.212	497.6	
kg BTX per kg dried biomass $(wt\%)$	3.368		

Table 18 – Summarized results from the energy balance over the gasifier unit

Inlet		Outlet	
Biomass	E_{S3} (MW)	Component	$E_{S4,i}$ (MW)
Total	0.8321	H_2	0.5038
Air	E_{S17} (MW)	CO	0.9241
Total	0	CO_2	0.6208
LHV of biomass (MW)		CH_4	0.2647
49.97		N_2	2.1835
Total energy in inlet (MW)		Water vapor	1.875
50.80			

Table 19 – Summarized results from the energy balance over the gasifier unit, continued

Outlet continued			
Component	$E_{S4,i}$ (MW)	Component	$E_{S10,i}$ (MW)
Benzene	0.0867	**Char**	0.1993
Toluene	0.0201	**Ash**	-
Xylene	0.0104	**Total**	0.1993
Naphthalene	0.0434	LHV of dry gas (MW)	
Total	6.537	28.48	
LHV of tar (MW)		LHV of char (MW)	
5.140		6.028	
Total energy in outlet (MW)		Net heat produced (MW)	
46.06		4.375	

4.3 Tar cracker

The reaction conditions, temperature and pressure, shown in

Table 20, FCC process were based on the experiments conducted by Pujro et al. [27], while the mass flow of tar into the reactor was calculated by mass balance over the gasifier. The tar was assumed as a mixture of heavy aromatic compounds, the composition used, being from Table 3. The selectivity and conversion were obtained from data provided by Pujro et al. and can be viewed in Table 11 and Figure 16 respectively [27].

Table 20 - Tar cracking process conditions.

Characteristics of inlet flow	Parameter values
Flow of tar	$0.138\ kg/s$
Temperature	450 °C
Pressure	$1\ bar$

The assumptions for this section of calculations include:

- The FCC process was assumed just as a single tube reactor and the regeneration process was neglected.
- The required air and steam were assumed to be coming with the producer gas and no additional inlets were considered.
- No conversion of producer gas occurred in the reactor.
- Concentration of tar in the inlet stream did not affect the conversion.
- No formation of coke occurred, and benzene was the only product of the reaction.
- The catalyst got completely regenerated throughout the FCC process

A flow scheme of the tar cracker used for the mass and energy balances is shown in Figure 22. It should be noted that due to time constraints, the calculations for tar recirculation were not done, but as will be explained further on, a pure stream of tar can be recirculated back to the tar cracker to produce more BTX.

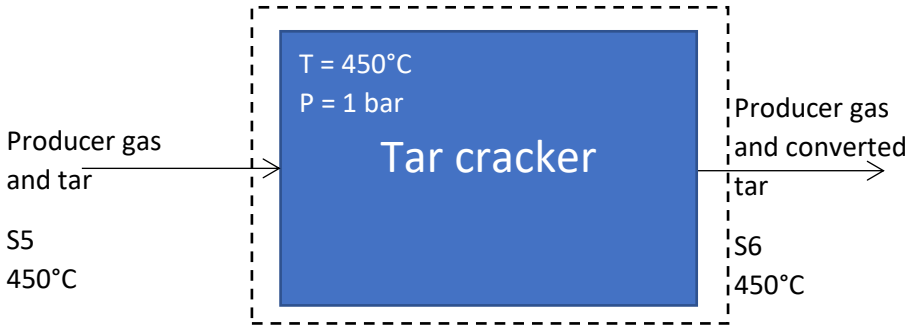

Figure 22 - Flow scheme of the tar cracker

The mass and energy flows of the inlet and outlet are presented in Table 21, indicating an increase of more than 9% in the quantity of benzene, which would get even higher if tar is recirculated back to the reactor.

Table 21 – Mass flow, energy flow and energy content of the tar in the inlet and outlet of the tar cracker

	Inlet			Outlet		
Substance	Mass Flow (kg/h)	Energy flow (MW)	Energy content (MJ/kg)	Mass Flow (kg/h)	Energy flow (MW)	Energy content (MJ/kg)
1-PhO	52.04	0.0093	0.6437	44.66	0.00799	0.6437
Biphenyl	15.20	0.0080	1.888	14.33	0.00751	1.888
Fluorene	15.20	0.0065	1.539	6.685	0.00289	1.539
9,10-DHP	15.20	0.0069	1.631	13.07	0.00592	1.631
Naphthalene	52.62	0.0262	1.793	47.07	0.02345	1.793
Phenanthrene	21.05	0.0112	1.920	17.68	0.00943	1.920
Pyrene	2.339	0.0012	1.902	1.127	0.00060	1.902
BaA	2.339	0.0014	2.101	0.8342	0.00049	2.101
Benzene	233.9	0.1189	1.830	264.3	0.1343	1.830
Toluene	58.47	0.0197	1.213	58.47	0.0197	1.213
Xylene	29.23	0.0073	0.893	29.23	0.00725	0.8930
Total BTX in	321.6	-	-	352.0	-	-
Total	497.6	0.2165	-	497.6	0.2196	-
Increase in BTX $(wt\%)$		9.468	Net heat consumed (MW)			0.00309

For the sizing of the reactor, the volume was calculated to be $27.23\ m^3$, with the height and the diameter being $36.53\ m$ and $0.9743\ m$ respectively.

4.4 Separation

4.4.1 Absorption

The mass and energy balances for the absorption process were done using Aspen Hysys V10. To simplify the simulation, several assumptions were made.

- All tar except BTX was approximated as naphthalene
- Absorption of water was neglected as TEG was found to have a low affinity to water for the present composition. The water was also found to not condense with the present conditions
- Several "virtual" units, heat exchangers and a separator were added, due to the addition of water to the purified gas mixture, instead of inlet gas
- The absorption process was run on adiabatic conditions

Figure 23 shows the overall simulation flow sheet. The fluid package used for this simulation was NRTL, with vapor model of RK. The number of stages was chosen to be 10. The results for the absorption unit can be viewed in Table 22.

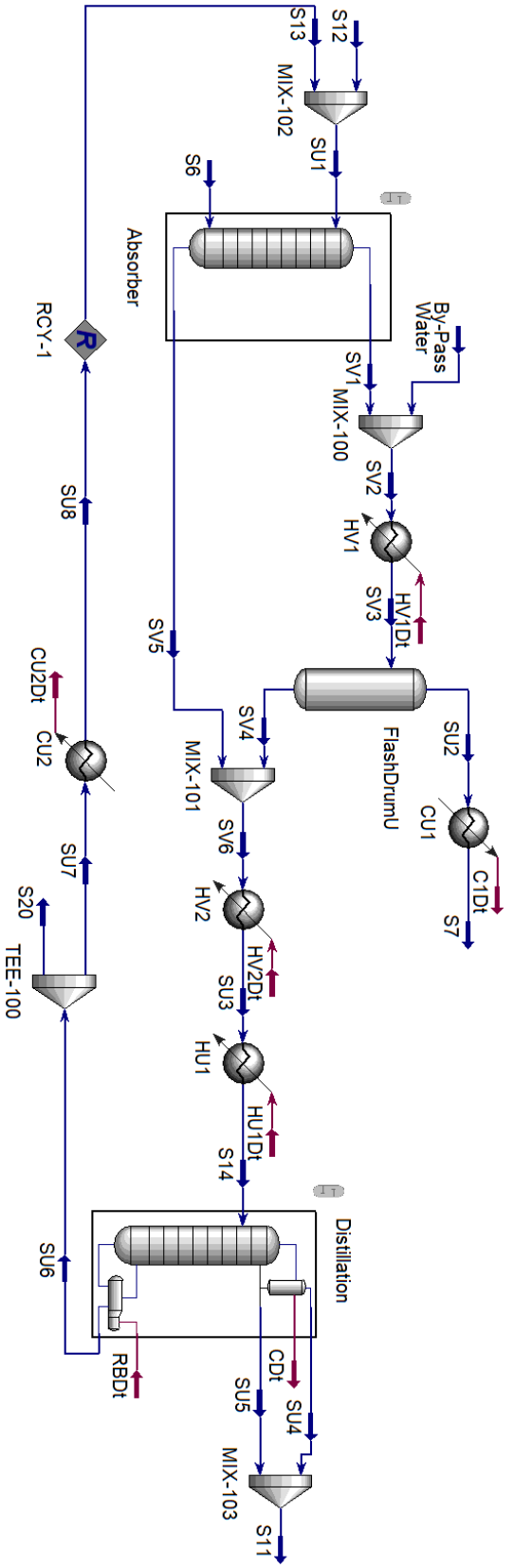

Figure 23 – Absorption and distillation columns flow sheet in Aspen Hysys environment

Table 22 – Absorption process streams

		$S6$ (kg/h)	$S12$ (kg/h)	$S13$ (kg/h)	$SU2$ (kg/h)	$SU3$ (kg/h)
Tar	Benzene	264.3	0	0	263.3	4.572
	Toluene	58.47	0	0	56.65	2.601
	Xylene	29.23	0	0	26.69	2.932
	Naphthalene	145.5	0	0.1307	0.1171	147.5
Producer Gas	H_2	172.5	0	0	172.5	0.002
	CO	2682	0	0	2682	0.0456
	CO_2	4172	0	0	4172	0.4348
	CH_4	602.2	0	0	602.2	0.0398
	N_2	10425	0	0	10425	0.2692
	H_2O	2227	0	0	2227	0.9717
Absorbent	TEG	0	120	932.7	1.290	1054
	Temperature (℃)	65	25	25	62.76	66.51

Several parameters were varied in order to achieve most tar removal, while using the least amount of absorbent.

- Inlet gas temperature – The absorption process was highly dependent on the gas temperature. The higher the gas temperature, the less effective the tar removal. As such, this parameter was chosen as low as possible, but still higher than the gas dew point, in order to ensure no condensation would occur.
- Inlet liquid temperature – As found for the gas inlet, higher liquid temperatures decreased the process efficiency, albeit much less compared to that of the inlet gas. It was also relatively ineffective on the temperature of the outlets, which could be attributed to the amount of liquid being low compared to the inlet gas. Nevertheless, it was assumed that TEG would enter the column at 25 ℃.
- Pressure – Less TEG would be required for absorption if the column was pressurized. Due to a higher dew point, the gas inlet temperature would need to be increased, decreasing tar absorption to some extent. However, as the other processes were under pressure of 1 bar, the same pressure was used.
- Mass of absorbent – The more TEG used in the column, the better removal of tar would be achieved. At some point though, increasing it further would result in more absorption of BTX, especially Xylene. The rate of recirculation and the make-up TEG could be optimized even further, to ensure less removal of BTX for unchanged absorption of naphthalene and smaller amount of inlet liquid.

4.4.2 Distillation

The distillation unit was required for the separation of tar from the absorbent, with the purified TEG being recirculated back to the scrubber, while the separated naphthalene could be led back to the tar cracker in order to get more benzene, or to the gasifier, to produce more energy. Table 23 shows the results of Aspen Hysys simulation of the distillation column.

Table 23 – Distillation process streams.

		$S14$ (kg/h)	$SU4$ (kg/h)	$SU5$ (kg/h)	$SU6$ (kg/h)
Tar	**Benzene**	4.572	4.4800	0.0925	0
	Toluene	2.601	2.515	0.0851	0
	Xylene	2.932	2.777	0.1552	0
	Naphthalene	147.5	111.9	35.41	0.1475
Producer Gas	**H_2**	0.002	0.002	0	0
	CO	0.0456	0.0456	0	0
	CO_2	0.4348	0.4344	0.0004	0
	CH_4	0.0398	0.0397	0	0
	N_2	0.2692	0.2691	0.0001	0
	H_2O	0.9717	0.9717	0	0
Absorbent	**TEG**	1054	0.4754	1.054	1053
	Temperature (℃)	250	210.2	210.2	277.9

As with the absorption column, the distillation tower used an NRTL fluid package, with RK vapor model. The feed, the liquid outlet of the absorber was heated up to the temperature of $250\ °C$. A partial condenser was used for the top product. This was due to the fact that the inlet stream had trace amounts of gases, meaning that the use of a total condenser, would require cooling the top product to negative temperatures. Using a partial condenser at temperature of 210.2 ℃ resulted in an almost complete separation of the tar from the absorbent, while the reboiler and the condenser complemented each other in terms of energy use. For distillation with a partial condenser, three degrees of freedom were available, allowing the user to put as many specifications.

- TEG recovery at the top outlet liquid, $SU5$ was 0.001 mass fraction.
- Naphthalene recovery at the bottom product, $SU6$ was 0.001 mass fraction.
- CO recovery at the top outlet vapor, $SU4$ was 0.999 mass fraction.

This allowed for an almost complete recirculation of the bottom product to the absorber. This, however, in combination with low amounts of make-up absorbent used for the absorption column, resulted in very high mass flow of TEG in the system, which would make the absorption process selective to water, as opposed to tar. Hence, more make-up and less recirculation were used, to keep the TEG flow in the absorber below water absorption limits. The products from the top of the distillation tower, $SU4$ and $SU5$ are both rich in naphthalene, and can be mixed, heated up and recirculated to the tar cracker. Table 24 shows the energy consumption in different parts of the absorption and regeneration processes, calculated by Aspen Hysys.

Table 24 - Results from energy balances over absorber and distillation column. Heat entering the system is defined as positive, and heat leaving as negative

Unit	Energy (MW)
Absorber	0
S14	0.1835
Recirculated TEG	-0.1976
Distillation condenser	-0.4592
Distillation reboiler	0.4928
Adsorption condenser	-0.0580
Net heat released (MW)	-0.0385

4.4.3 Activated carbon adsorption

The operational parameters for the activated carbon bed were fixed at 55 ℃ temperature and $1\ bar$ pressure.

Donau Carbon was chosen as a potential supplier of activated carbon. The company suggested Desorex K43 as the most appropriate activated carbon for BTX adsorption, and Table 25 presents Desorex K43 specifications.

Table 25 - Desorex K43 specifications [37]

Bulk density (kg/m^3)	470 ± 30
Moisture content	$< 8\ wt\%$
Total surface area (m^2/g)	1000
Diameter of particles (mm)	4
CTC-adsorption	$> 60\ wt\%$
$C_{p\ bed}\ (kJ/mol, K)$	0.84 [1]
Adsorption capacity of benzene at $55\ °C$ at $p/p* = 0.9$	0.38 [2]

The assumptions for the mass and energy balances were:

- No energy gas will get adsorbed to the activated carbon.
- BTX are treated as benzene when applying data from Donau Carbon.
- Since activated carbon generally has a low heat transfer coefficient – between $0.65 - 0.85\ W/m.K$ – there is assumed to be no hot spots or burning of carbon in the bed.
- The amount of BTX that is irreversibly adsorbed is neglected.
- Desorption temperature for BTX on Desorex 43 is 130 ℃ according to Donau Carbon, but a heating to 200 ℃ decreases the small amount still not desorbed at 130 ℃.

Since naphthalene will get adsorbed onto the activated carbon easier than BTX, according to Donau Carbon, 100% of the naphthalene was assumed to be adsorbed. Figure 24 and Figure 25 below present the mass and energy flows over the activated carbon bed, where the inlet gas stream S7 was the producer gas from the scrubber. The first step is the adsorption of BTX and naphthalene from the producer gas. The adsorption step is exothermic, i.e. heat is generated during the process, and this heat is used to produce district heating. The energy gas is not adsorbed in the process and therefore goes straight through and is subsequently sent to the boiler in the CHP-section. When the activated carbon is saturated with BTX and naphthalene, the producer gas stream is switched to the other activated carbon columns while desorption the newly saturated column is initiated. The desorption step is endothermic, which implicates energy needs to be added. This heat is taken from 20% of the steam produced in the CHP section.

[1] Retrieved from Donau Carbon employee Ulli Riedelbach

[2] Extrapolated between 20 and 35°C

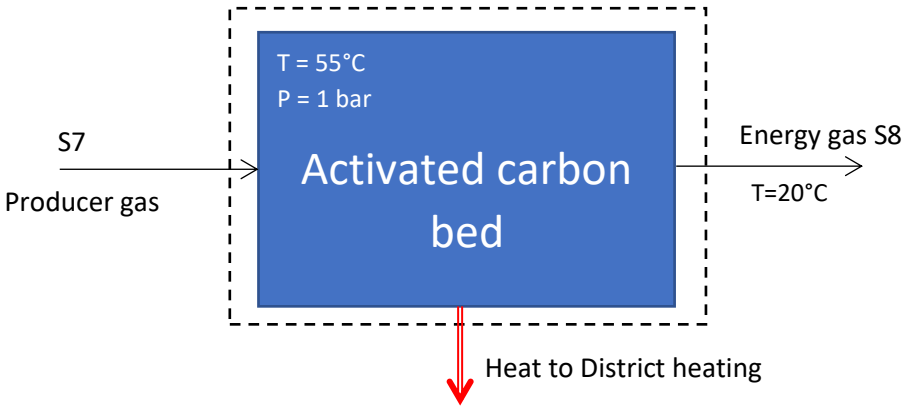

Figure 24 – System boundary for mass and energy balance for the adsorption step over the activated carbon bed

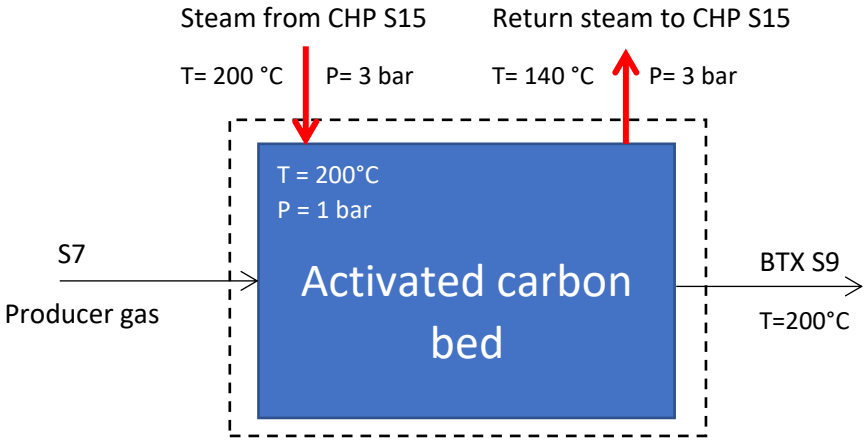

Figure 25 – System boundary for mass and energy balance for the desorption step over the activated carbon bed

Table 26 presents the mass flows for the inlet and outlet gas steam for the activated carbon bed.

Table 26 - Mass flows, inlet and outlet gas steam of the activated carbon bed

Component	**Inlet gas stream, S7 (kg/h)**	**Outlet gas stream, S8 (kg/h)**	**Adsorbed gas, S9 (kg/h)**
Naphthalene	0.117	0	0.117
Benzene	263.3	9.214	254.1
Toluene	56.65	1.983	54.67
Xylene	26.69	0.934	25.75
H_2O	2227	2227	0
CO	2682	2682	0
CO_2	4172	4172	0
N_2	10425	10425	0
H_2	172.5	172.5	0

CH_4	602.2	602.2	0
Total	**20627**	**20292**	**334.6**
BTX production per year $(kg/year)$			**2819000**
BTX fraction of S9 $(wt\%)$			**99.97**
BTX fraction lost in S8 $(wt\%)$			**3.50**

A purity of $99.97\ \%$ was attained, which is the amount of BTX in relation to the total amount of adsorbed gas. The adsorbed gas is as explained then desorbed and stored as the final product.

Table 27 shows the result for energy balance for the adsorption and desorption steps in the activated carbon bed.

Table 27 – Energy balance for adsorption and desorption steps in the activated carbon bed

Adsorption step	Heat generated/Cooling duty (MW)	0.075
	Cooling water mass flow (kg/h)	2152
	Time required for the adsorption of BTX and naphthalene (h)	6
Desorption step	Total heat required (MW)	0.331
	Steam flow from CHP (kg/h)	9433
	Time required for the desorption of BTX and naphthalene (h)	5.43

As a result of the mass and energy balances it was found that the activated carbon bed consists of two columns in parallel for adsorption and two columns for desorption respectively, totaling four columns. Column specifications and size are shown in Table 28. Time of the adsorption of BTX and naphthalene is a function of the size of the column, i.e. the weight of the activated carbon. The size of the columns was chosen in order to have time of adsorption of BTX and naphthalene close to $6\ hours$. A higher time would increase the investment cost, since it would require larger columns.

The time for BTX and naphthalene desorption is a function of the steam flow from CHP, so the steam flow chosen in order to have approximate $5-6\ hours$ for desorption for the reason to have some extra time (quarter of an hour) to fully drive out all the desorbed gas until the columns are switched to adsorption step. This chosen steam flow was later implemented in the CHP-calculations described in section 4.5.

Table 28 - Activated carbon column´s size and specifications

Total columns specifications	Number of columns	4
	Total volume (m^3)	25.36
	Adsorption efficiency (%)	96.5 [36]
	AC Weight (kg)	11920
Column size	Diameter (m)	1.391
	Height (m)	4.173
	Surface area (m^2)	18.23

In summary, for $6\ hours$, two activated carbon columns get saturated from the BTX in the producer gas, while the other two gets desorbed.

4.5 Combined heat and power

The composition of the energy gas that was used in the boiler was the same as the outlet gas that leaves the activated carbon bed. The system boundary for the mass and energy balances are shown in Figure 26.

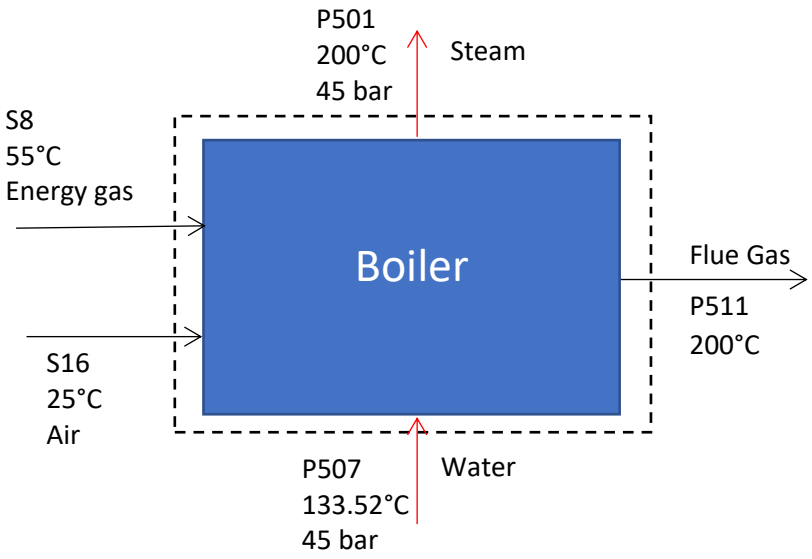

Figure 26 - System boundary for mass and energy balance over the boiler

The amount of air was calculated assuming 120 % of excess for the combustion reactions of methane, benzene, toluene, xylene, and hydrogen was assumed. Complete combustion was assumed for the mass balance around the boiler. A summary of the obtained results for inlet and outlet stream around the boiler is shown in Table 29.

Table 29 – Results from mass balance around the boiler

Stream	**Energy gas (S8)**		**Air (S16)**		**Flue gas (P510)**	
	(kg/h)	(mol/s)	(kg/h)	(mol/s)	(kg/h)	(mol/s)
H_2	172.5	23.96	-	-	-	-
CO	2681	26.60	-	-	-	-
CO_2	4171	26.34	-	-	5910	37.32
CH_4	602.1	10.45	-	-	-	-
N_2	10425	103.4	21166	209.99	31592	313.4
H_2O_{fuel}	2227	34.36		-	2226	34.36
Benzene	9.214	0.0328	-	-	-	-
Toluene	1.983	0.0060	-	-	-	-
Xylene	0.9341	0.0024	-	-	-	-
O_2	-	-	6430	55.82	1109	9.628
	-	-	-	**H_2O_{rx}**	2916	45.004
				H_2O_{total}	5143	79.37

The energy balance was completed considering the combustion reactions at 25 °C, the energy that the energy gas adds to the system, and the energy that the flue gas takes out of the system. A boiler efficiency of 80 % was considered [75].

It was calculated that the boiler could deliver $31.32\ MW$. With this amount of energy, the mass flow of steam the can be produced was $37575\ kg/h$.

Figure 27 and Figure 28 show the system boundaries for the calculations around the turbines.

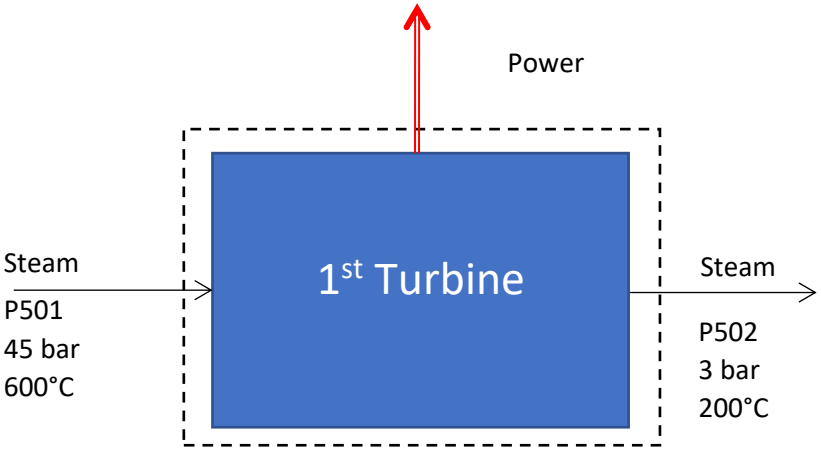

Figure 27 - System boundary for mass and energy balance over the 1st Turbine

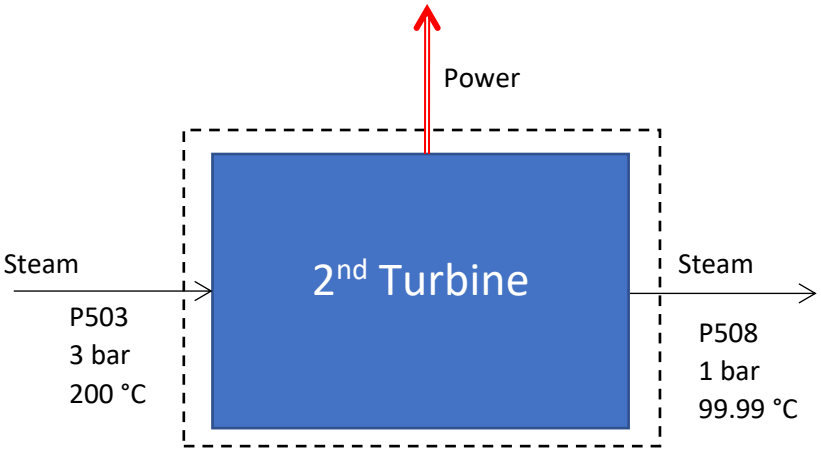

Figure 28 - System boundary for mass and energy balance over the 2nd Turbine

Table 30 and Table 31 show the results from the mass and energy balances around the combined heat and power section.

Table 30 - Results from energy and mass balance of steam in CHP section

	Physical state	Mass flow (kg/h)	Pressure (bar)	Temp $(°C)$	Enthalpy (kJ/kg)	Entropy $(kJ/kg.K)$	Note
P501	Superheated steam	37574	45	600	3550.2	73.13	Pressure from U.S. department of energy [42]. T calculated as isentropic case of P502
P502	Superheated steam	37574	3	200	2865.9	73.13	T and p based on desorption process needs
P503	Superheated steam	28140	3	200	2865.9	73.13	Split current. Same T and p as P502
P504	Superheated steam	9433.5	3	200	2865.9		Split current. Same T and p as P502
P505	Superheated steam	9433.5	3	140	2739.4		T and p based on desorption process needs
P506	Saturated liquid	9433.5	3	133	561.40		T of saturated liquid
P507	Liquid	9433.5	45	133	549.30		Same p as steam in boiler output
P508	Superheated steam	28140	1	100	2657.9	73.13	T calculated as isentropic case of P502
P509	Saturated liquid	28140	1	99.6	417.50		T of saturated liquid
P510	Gas	43755	1	200	6288.1	Enthalpy in kW obtained from Flue Gas enthalpy calculator	
P511	Gas	43755	1	108	5025.9		

Table 31 – Results from energy and mass balance of steam in CHP section continued

Section of CHP Process	Energy (MW)
District heating from flue gas cooling	1.26
District heating from steam condensing after desorption	5.71
District heating from steam condensing after 2nd turbine	17.51
Power Output from 1st Turbine	7.14
Power Output from 2nd Turbine	1.63

The results for the heat and power output as well as the efficiency of the system are shown in Table 32.

Table 32 - Energy delivered by CHP process

	Energy (MW)	Efficiency
Total district heating from steam	24.48	0.87
Total Power Output	8.16	0.29
Total CHP Output	32.64	1.16

5 Economics

The potential profitability for the plant has been calculated using the Net Present Value (NPV) method with an order of magnitude of $\pm 30\%$ based on previous cost estimations [76]. Direct costs and indirect costs have been summarized resulting in the Fixed Capital Investment (FCI), Working Capital Investment (WCI) and Total Capital Investment (TCI). The annual income is based on sales of bio-char, district heating, power and BTX. Accounting for constant inflation of $2.06\ \%$ and a discount rate of $5\ \%$ the NPV was found to be $48\ MSEK$ after 15 years of initial investment. The total equipment costs of the plant are summarized in Table 33.

Table 33 – Summary of equipment costs

Equipment	Price $(MSEK)$
Biomass Handling	61
Gasifier	74
Hot Gas Filter	4
Tar Cracker	1
Scrubber	0.27
Distillation	0.45
Adsorption (Carbon beds)	1
CHP	36
Heat Exchangers/Condensers	1
Pumps & Fans	1
BTX Storage	0.38
Total	**180 *MSEK***

The remaining direct and indirect costs were calculated by relating to the total equipment cost. The direct and indirect costs are presented with the corresponding percentage rate [77] in Table 34 and Table 35 respectively.

Table 34 – Summary of direct costs

Direct Costs	Percentage rate (%)	Price $(MSEK)$
Equipment	100	180
Installation	47	85
Instrumentation & Controls	36	65
Piping	68	122
Electrical	11	20
Building, Process & Auxiliary	18	32
Service	70	126
Land	10	18
Total		**648 *MSEK***

Table 35 – Summary of indirect costs

Indirect Costs	Percentage rate (%)	Price $(MSEK)$
Engineering	33	59
Legal Fees	4	7
Construction &Constructors Fee	63	113
Contingency	44	79
Total		**259 *MSEK***

The annual income is presented in Table 36 and the prices are taken from sources [78] [79] [80] [81]. The plant is considered to run full-time with an exception for two weeks of down time (total operating

time is $8424\ hours/year$). The operating expenses are calculated based on the GoBiGas plant [82] and are presented in Table 37.

Table 36 – Summary of annual income

Product	Production	Price	Income $(MSEK/year)$
Bio-char	$5796\ ton/year$	$12\ SEK/kg$	70
District Heat	$293\ GWh/year$	$804\ SEK/MWh$	236
Power Production	$68\ GWh/year$	$463\ SEK/MWh$	32
BTX	$2862\ ton/year$	$11.48\ SEK/kg$	32
		Total	$\mathbf{369\ MSEK/year}$

Table 37 – Summary of operating expenses excluding biomass and TEG

Operating cost	Cost (SEK/MWh)
Personnel	190
Maintenance	123
Consumables (Excluding biomass and TEG)	130
Other Costs	37
Total	$\mathbf{480\ SEK/MWh}$

$$\text{Fixed Capital Investment (FCI)} = \text{Direct costs} + \text{Indirect costs} = 906.7\ MSEK$$

$$\text{Working Capital Investment (WCI)} = 10\%\ FCI = 91\ MSEK$$

$$\text{Total Capital Investment (TCI)} = FCI + WCI = 997\ MSEK$$

To add further to Table 37, the operating expenses including biomass and TEG costs were calculated to be 281 MSEK/year. Furthermore, to provide a basic idea of plant profitability, Return on Investment (ROI) before tax was chosen as one of the points of discussion [76].

$$\text{ROI (before tax)} = 8.89\%$$

Based on estimates for new process development from Dow Chemical [83], a reasonable value would be 30% for ROI. A value of 8.89% indicates a risk for future process development based on this concept.

The NPV was calculated as the difference between the investment cost and the future net cash flows for a 15 year period. The total investment cost consists of the FCI and the WCI (10% of FCI) [84] and the net cash flow is the difference between the annual income and the operating costs including the costs for biomass and TEG. Finally, a sensitivity analysis was made for the NPV at the 15th year, altering the income, expense, the investment cost and the discount rate separately. The effects on the NPV of each variable are presented in Figure 29.

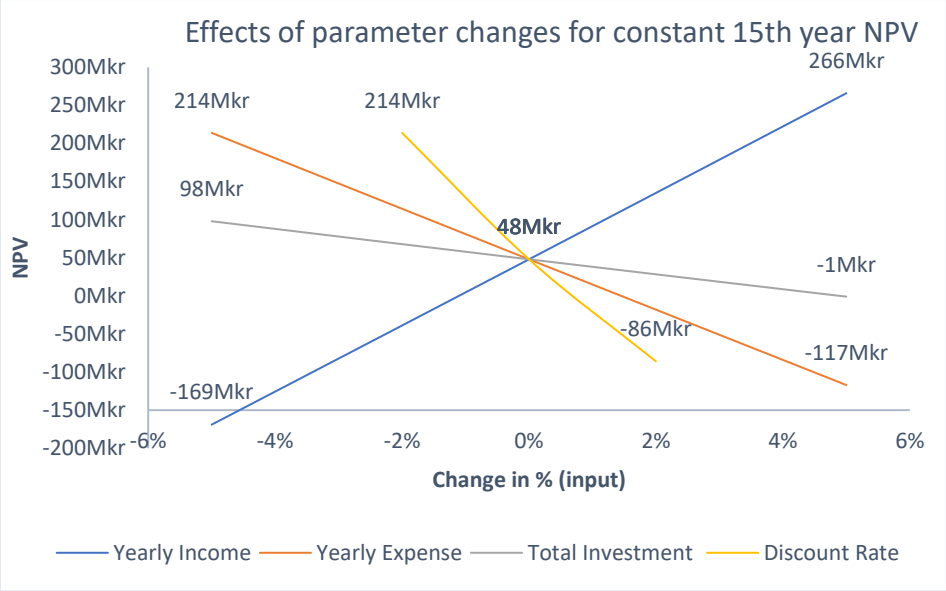

Figure 29 - Sensitivity analysis of the net present value at the 11th year of the project

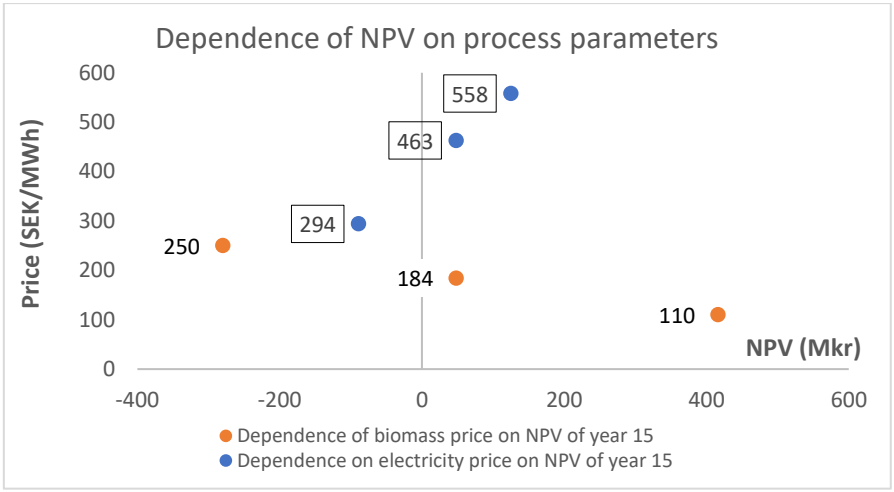

Figure 30 - Net present value dependence on biomass and electricity price

Indicators of profitable plant operation (NPV) were investigated by varying biomass and electricity prices as seen from Figure 30. Firstly, electricity price was kept constant at $464\ SEK/MWh$ to find NPV by varying biomass price. Secondly, biomass price was kept constant at $184\ SEK/MWh$ to find the same by varying the electricity price. It is noted that the plant profitability (described by a positive value of NPV) is available at the present value of biomass and also when the biomass price fell to a significantly low value of $110\ SEK/MWh$. Also, a higher price of electricity pushes the trend towards a positive NPV value. The present value ($463\ SEK/MWh$) or a higher value of electricity price from Nordpool [80] renders the plant operation to become profitable for year 15, which denotes the maximum service life for most of the unit processes. When considering the biomass price, a larger value shifts the trend towards a more negative NPV value. Therefore, the primary observation would be that biomass price is more critical in determining profitable operation, when compared with electricity income generated.

6 Discussion

Considering the biomass availability, possibility for extraction and transport, a suitable location to set up the plant would preferably be the south of Sweden. Southern Sweden holds potential for a larger harvesting area and the concerns arising out of large transportation distances for the harvested biomass are avoided. Figure 31 illustrates a comparison of biomass extraction for north and south of Sweden. Here, the term 'northern' refer to Norrland and 'southern' refers to Götaland and Svealand. Furthermore, GROT (slash) extraction from the south of Sweden is an option that can be considered in this context, without much consideration on any other economic criteria tied to biomass import or long-distance transportation.

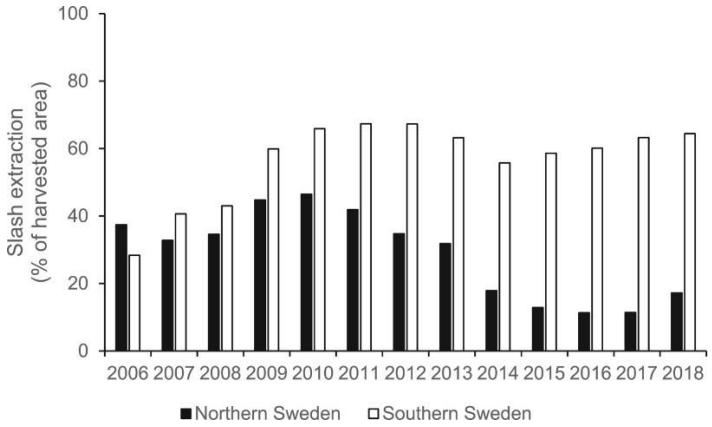

Figure 31 - Comparison of possibility in biomass extraction for northern and southern Sweden [85]

As for the process design, the pre-treatments were dependent on both the choice of biomass and the gasifier technology. While CFB was reported to tolerate up to $15\ wt\%$ moisture content of biomass, Arthur M. James R. et al. reported a significant increase in tar content as well as biochar in reducing the moisture content from $18\ wt\%$ to $10\ wt\%$ [86], albeit in an updraft gasifier. While they did not study potential changes in tar composition, these results showed that increased drying would be warranted for production of BTX. While drying the biomass to a moisture content below $8\ wt\%$ would require more energy, this could also prevent issues related to moisture condensation in the separation and conditioning processes as well as increase the LHV of the energy gas for CHP.

Gasification was probably the most crucial and limiting part of the entire process. Table 17 showed that with the applied data, only $5\ wt\%$ of the biomass formed tar, and as low as $3\ wt\%$ formed BTX, which is not very promising as the main objective of the process was to produce BTX. The low conversion is connected to the tar yield given in Table 9, which not only was taken from a BFB gasifier, but also with temperatures between $780 - 830$ ℃ and air as a gasifying agent. As mentioned, this data was chosen due to lack of detailed alternatives, since most present studies on gasification focus on minimizing tar production and not maximizing it, so the process could probably be optimized to produce both more tar and BTX. This could e.g. be by using a CFB gasifier with silica sand, lower temperatures, possibly steam injection, and possibly even a pressurized system, but this would have to be investigated in detail in a laboratory study. Another factor that would have to be investigated in conjunction with this would be the reaction kinetics.

Looking back at Table 18, a net heat release of $4\ MW$ was calculated, with most of the energy of the biomass being stored in the energy gas. This heat is probably much lower in reality, as the distribution of products in the outlet likely differ a lot. In particular, reactions (1)-(3) might happen to smaller extents, and more heat could be stored in the many tar compounds not considered in this study. On

the other hand, if these reactions happen to a large extent in practice ER could be reduce further and/ or steam could be injected in order to control the temperature of the gasifier.

The zeolite catalyst in the tar cracker was mainly chosen for its high selectivity. However, as was seen in Figure 16, its conversion was relatively low, which is why the BTX only was increased by $9.5\ wt\%$ as presented in Table 21. This low conversion would require a lot of tar to be recirculated, but seeing as the tar flow was relatively low compared to the energy gases, this should not prove to be a problem. The study from which the catalyst data was gathered was performed with a laboratory scale reactor only simulating the riser section of the FCC process, shown in Figure 17, so the conversion might differ for a large-scale process.

Other catalysts showed much higher conversion with greater selectivity than E-Cat used in the FCC process. The problem, however, was the need to pressurize the whole process which made this option an unattractive one. On the other hand, high conversion of tar to BTX would increase its production, meaning that recirculation would probably not be needed either. The separation processes would also change in this case, due to low amounts of tar in the tar cracker's outlet. An absorption column to separate BTX from the producer gas would be much more efficient in such pressures than atmospheric ones, but using an activated carbon bed, as was done in this project, would still be possible. Using elevated pressures would introduce other problems though, such as expensive compressors, higher dew points, material constraints and possibly safety risks.

The coke formation in the tar cracker was neglected, and the tar which would have formed coke was assumed to not react at all. This means that the calculated tar flow was slightly overestimated, and if the recirculation would have been added, the production of coke would reach a point where it has to be considered. While this would yield a higher increase in BTX, the production would still be limited as there would be an unavoidable loss of tar. On a side note, as the coke would be combusted this would also give a higher energy production, compared to the present case where *0.003 MW* of energy is *consumed*.

As for the absorption and regeneration process, it can be noted from Table 22 that the simulation was successful in removing almost all the tar (naphthalene) in the inlet gas stream by using TEG. Furthermore, addition of water to the inlet gas stream with the current amount of TEG did not result in its absorption, and only by increasing the TEG into the process by at least 1.5 times could any water be absorbed into the liquid. It was concluded that despite the fact that TEG is a highly effective gas-drying means [87], the gas was already dry enough, so that water would not affect the absorption process. This conclusion was of high importance to the simulation, because the absorption column would not be able to converge in the presence of water.

The problems with water in the separation processes were partly why the biomass was dried despite already having a moisture content below $15\ wt\%$, and partly why steam injection was not considered for the gasifier. As with any simulation though, reality might differ significantly, and in order to ensure that no water would be absorbed and to validate the use of TEG, this would have to be tested in practice. If water would prove to be absorbed, one of the drying processes mentioned in section 3.5 could be employed before tar-absorption. As the water would be removed, Table 22 and Table 23 showed that a high recovery of tar could be achieved in the absorber, and a large amount of TEG could be recirculated after distillation, respectively.

As for the calculated energy requirements showed in Table 27, these proved to be relatively low when compared to other processes, and this is probably due to the small mass flows of tar and TEG. If the tar yield was increased, all of the separation processes would probably be more energy intensive, as

more tar would have to be absorbed and probably require more TEG, which would then have to be separated in the regeneration.

The results for the adsorber in Table 26 showed a purity of $99.97\ \%$ BTX in the desorbed gas, with the rest being residual naphthalene corresponding to the remaining tar. This is a very high purity, and it is due to the high removal of tar in previous separation processes, along with the lack of adsorption of the energy gases.

Only $3.5\ wt\%$ of the BTX was lost with the energy gas, though this is when the activated carbon is also considered as fresh. Over time, this loss will likely increase as the performance of the activated carbon will deteriorate over time, due to attrition. It is also questionable whether all energy gas goes straight through the adsorption bed without some small amounts getting trapped. In particular, small amounts of methane could get adsorbed in the bed, resulting in slightly lower purity of the BTX.

The heating and cooling duties shown in Table 27 were relatively low compared to other unit processes. The calculation for the cooling duty due to heat of adsorption could be too simplified as no heat transfer equations were used, so the real cooling duty may be larger. Conversely, the heating needed for the desorption might in fact be higher as it uses same coil jacket. The option of doing steam regeneration, i.e. add steam directly to activated carbon bed, would give a faster time for desorption [40], but as of now there is no need to improve the time for desorption as it is sufficiently fast. The steam regeneration would also add an additional separation step to separate the steam from the BTX, which could prove to be more costly in the end.

One decision in the process design was to neglect pressure drops, and this is a factor that in reality likely would reduce the net electricity produced significantly. In order to drive the various flows throughout the process, both fans and pumps would have to be placed, were especially the fans would drain a lot of the electricity the turbine provides. This could also mean that the second stage of the turbine, where the steam expands from 3 bar to 1 bar, would not be possible in reality as the pressure is needed to drive the flow of steam. Elevated pressures from the fans could also increase the dewpoint of some of the gas mixtures, which would have to be counteracted by increasing the temperature of the affected streams.

Finally, Table 31 and Table 32 showed that relatively high amounts of district heating were produced from the CHP process. The total amounts of heat and power obtained from the process were $24.48\ MW$ and $8.16\ MW$ respectively. The thermal efficiency of the system with relation to LHV was 87%, and the electrical efficiency was 29%. The overall efficiency, which was 116%, was higher than 100% due to the fact that flue gas was cooled after leaving the boiler, and it could have been higher if flue gas condensation was further analyzed.

The electrical efficiency obtained in this project is acceptable according to data provided by the Royal Swedish Academy for Engineering Sciences which states that CHP plants that use biofuel usually have electrical efficiencies between 25 and 28% [88]. However, according to a report performed by the company Ricardo-AEA Ltd for the European Commission, the electrical efficiency of plants that use wood fuels (including wood chips), is in the range from 21% to 39%. The efficiency of this project is in the low part of this range, and the reason can be that the gasifier was used in an inefficient way since the main goal of the study was to maximize the production of tar and obtain BTX from it. The same study recommends a reference thermal efficiency of 86%, therefore, the thermal efficiency obtained in the CHP section of the project is acceptable [89].

The possibility of district heat production was evaluated and quantified. Table 38 indicates an estimate of the net heat available for supply to district heating grid after its localized use for heating atmospheric air for biomass drier unit.

Table 38 – District heat production capacity

Heat Exchanger Data	Energy (MW)
CHP Heat Exchanger 1	5.71
CHP Heat Exchanger 2	17.51
FGC Heat Exchanger 3	1.26
Heat from gasifier	4.03
Jacketed adsorber coil	0.07
Pre-BTX storage Heat Exchanger 4	0.02
Gasifier-Cracker Heat Exchanger 5	2.6
Cracker-Absorber Heat Exchanger 6	3.0
Scrubber-Distillation Heat Exchanger 7	0.71
Total heat available for extraction	**36.33**
Heat utilized for biomass-drying	1.53
Net heat available for district heating	**34.8**

One of the main design choices of the process was to neglect pressure drops. In reality, fans and pumps would have to be added to drive the various flows, which would reduce the net power produced. The second stage of the turbine would probably not be possible, as expanding the steam from a pressure of 3 bar to 1 bar would leave no pressure left to drive the flow, resulting in even lower power production. Elevated pressures due to the fans could potentially also introduce issues because of higher dew points of certain gas mixtures, and this might require some streams to be heated to higher temperatures in order to avoid condensation.

Considering that the lifetime of the plant is 15 years (25 years for gasifier and CHP) and that the net present value becomes positive during the last year before reinvestment is needed, this investment is not economically viable. To make a project like this feasible the income must increase, and the expenses should decrease, which could be achieved through some of the improvements and investigations for the different units, suggested earlier. Cheaper production of BTX together with increased demand, hence increased sale price would be of great benefit for this project. However, the risk of increased price of biomass has to be considered since it has a big impact on the NPV, as seen in section 5. The produced biochar and the TEG extracted from absorber recirculation could be sent to the boiler in the CHP section to increase the energy output, but the economic effect of this would have to be investigated further by comparing the income from the extra energy to the income from selling the biochar.

7 Conclusions

The study showed that gasification with a CFB gasifier could be used to produce BTX. An FCC tar cracker could be used to increase the production of benzene, and TEG could be used as an absorbent to recirculate a large portion of the unreacted tar, using distillation as a regeneration method. As the remaining gas contains BTX, an activated carbon absorber could be used to extract a relatively pure mixture of BTX, while the energy from the remaining gas could be extracted through CHP. Ultimately, with the assumptions made, this would yield a power production of $68\ GWh/year$ and a district heating of $293\ GWh/year$.

As the NPV would not be positive until after 15 years, the process was concluded to not be feasible for investment unless the processes are optimized further with more reliable data and models, and the demand of renewable BTX increases to a point where the selling price increases substantially.

8 Appendix

8.1 Pre-treatment calculations

The heat demand needed for drying the biomass feed to the desired moisture content is a necessary calculation step. Steps provided below describe the details needed for calculating drying-time and energy consumption of the drier as described in sources [51] and [52] .

Step 1: Calculating drying-time/residence time for biomass particles

Drying time $t = \frac{-x_p^{1.52}}{b} ln\left(\frac{W-W_e}{W_0-W_e}\right); b = 0.0575 + 0.00142\, p_w$ (11)

Here, $p_w = 20.41 - \frac{5132}{T\,(K)}; T = 298\ K$ (12)

p_w = vapor pressure of water (mm Hg)

x_p = particle thickness (inches); x = 2 cm = 0.8 inch

W = Average moisture content; $\frac{13.3+8}{2}$ = 10.65 %

W_e = Equilibrium moisture content [90] = 9.1 %

W_0 = Initial moisture content = 13.3 %

$\Rightarrow$ This in turn, provides a drying time of t = 11.45 seconds

Step 2: Calculating energy consumption for the drier

(A) Amount of heat energy required to evaporate moisture,

$Q_1 = F(X_{M,i} - X_{M,f})\left[r_0 - \left(C_{pw} - C_{pv}\right) T_D\right]$ = 0.29 MW (13)

F = Feed flow rate = 2.81 kg/s

$X_{M\,i}$ = Initial moisture content $kg/kg_{dry\ basis} = 0.133$

$X_{M\,f}$ = Final moisture content $kg/kg_{dry\ basis} = 0.08$

r_0 = Latent heat of vaporization of water at 25 °C $= 2441.7$ kJ/kg

C_{pw} = Specific heat of water at 25 °C

C_{pv} = Specific heat of water vapor at 230 °C

T_D = Drying temperature (assumed to be the same as air inlet temperature) = 230 °C

(B) Amount of heat energy required to heat wood chips to target temperature,

$Q_2 = F\left[C_{ps} + (X_{M,i}\, C_{pw})\right](T_D - T_0)$ = 1.09 MW (14)

C_{ps} = Specific heat of biomass at 25 °C $=$ 1.341 kJ/kg C

T_0= Ambient air temperature = 25 °C

(C) Amount of heat energy required to heat the air to target temperature,

$Q_3 = F_a\left[C_{pa} + \left(Y_0\, C_{pv}\right)\right](T_D - T_0) =$ 0.15 MW; $F_a = \frac{W}{\Delta Y}; W = F(X_{M,i} - X_{M,f})$ (15)

F_a = Flow rate of air required to dry biomass to target moisture levels = $11.7\ \mathrm{kg/s}$

ΔY = Humidity difference between ambient air and drying air = 58%

Y_0 = Ambient air humidity = 88%

C_{pa} = Specific heat of air at 230 °C

$\Rightarrow$ Total amount of heat energy required for drying = (A)+(B)+(C) = $1.53\ \mathrm{MW}$

8.2 Gasifier calculations

Firstly, the oxygen needed for all carbon in the biomass to form CO_2, and all the hydrogen to form H_2O was calculated through stoichiometry:

$$M_i = \frac{m_i}{n_i} \Leftrightarrow n_i = \frac{m_i}{M_i} \tag{16}$$

$$n_{O_2,stoich} = 2\frac{F_{S3,C}}{M_C} + \frac{1}{2}\frac{F_{S3,H}}{M_H} - \frac{F_{S3,O}}{M_O} \tag{17}$$

Using the assumed air composition, this yielded the stoichiometric air flow:

$$n_{air,stoich} = \frac{n_{O_2,stoich}}{0.21} \tag{18}$$

This flow was multiplied by the chosen $ER = 0.25$ to yield the applied air flow S17, in accordance with equation (9).

Secondly, a nitrogen balance was set up over the system boundary shown in Figure 21, neglecting the nitrogen in the biomass:

$$F_{S17,N_2} = F_{S4,N_2} \tag{19}$$

The gas composition shown in Table 9 was renormalized after excluding C_2H_n. F_{S4,N_2} was then used with the molar fractions to calculate the dry and tar-free gas molar flow, and the mass flow of H_2, CO, CO_2 and CH_4, respectively.

$$F_{S4,dry\ and\ tar-free} = \frac{F_{S4,N_2}/M_{N_2}}{x_{N_2}} \tag{20}$$

$$F_{S4,i} = F_{S4,dry\ and\ tar-free} \cdot x_{S4\ gas,i} \tag{21}$$

The ideal gas law was used to calculate the volumetric flow corresponding to $F_{S4,dry\ and\ tar-free}$

$$pV = nRT \Leftrightarrow V = \frac{nRT}{p} \tag{22}$$

With the help of equation (22), the volumetric flow was calculated in terms of normal cubic meters, defined at 0°C and $1\ atm$:

$$\frac{pV}{RT} = \frac{p_n V_n}{RT_n} \Leftrightarrow V_n = \frac{T_n R}{p_n} \cdot n = \frac{273.15 \times 8.314}{101325} \times n$$

where V_n is the volumetric flow of the dry and tar-free gas in terms of Nm^3. Referring to the tar yield in Table 9, V_n was used to calculate the tar flow $F_{S4,tar}$ and the mass flow of each tar component was calculated using the composition presented in Table 4:

$$F_{S4\ tar} = V_n \times 30 \tag{23}$$

$$F_{S4\ tar\ i} = F_{S4\ tar} \cdot x_{S4\ tar\ i} \quad (24)$$

Next, a molar balance of hydrogen was set up over the gasifier to estimate the amount of water vapor:

$$\frac{F_{S3,H}}{1} + 2 \cdot \frac{F_{S3,H_2O}}{18} = 2 \cdot \frac{F_{S4,H_2}}{2} + 4 \cdot \frac{F_{S4,CH_4}}{16} + 2 \cdot \frac{F_{S4,H_2O}}{18} + \frac{F_{S4\ tar,H}}{1}$$

$$\Leftrightarrow F_{S4,H_2O} = 9 \cdot \left(F_{S3,H} + \frac{F_{S3,H_2O}}{9} - F_{S4,H_2} - \frac{F_{S4,CH_4}}{4} - F_{S4\ tar,H}\right) \quad (25)$$

In which $F_{S4\ tar,H}$ is the total mass of hydrogen contained in the tar compounds. Note that the mass flows were divided by the corresponding molecular mass for each compound. The hydrogen of the tar compounds was calculated through stoichiometry; for instance, naphthalene has the molecular formula $C_{10}H_8$, which yields the following amount of hydrogen:

$$F_{S4\ Naph,H} = 8 \cdot \frac{F_{S4,Naph}}{M_{Naph}}$$

This calculation was repeated for all compounds in the tar model, yielding $F_{S4\ tar,H}$ and ultimately F_{S4,H_2O} through equation (25).

In a similar fashion, a molar balance of oxygen was performed:

$$\frac{F_{S3,O}}{16} + \frac{F_{S3,H_2O}}{18} + \frac{F_{S17,O_2}}{32} = \frac{F_{S4,CO}}{28} + 2 \cdot \frac{F_{S4,CO_2}}{44} + \frac{F_{S4,H_2O}}{18} \quad (26)$$

Equation (26) showed that slightly more oxygen was entering the gasifier than leaving, and this was likely due to errors in the assumed composition of the dry and tar-free part of S4. To compensate for this, the residual oxygen was assumed to form CO_2, which only increased the fraction of CO_2 in S4 very slightly.

Finally, similarly to the hydrogen balance, a carbon balance was set up over the gasifier to yield the char produced:

$$\frac{F_{S3,C}}{12} = \frac{F_{S4,CO}}{28} + \frac{F_{S4,CO_2}}{44} + \frac{F_{S4,CH_4}}{18} + \frac{F_{S4\ tar,C}}{12} + \frac{F_{S10,char}}{12}$$

$$\Leftrightarrow F_{S10,char} = 12\left(\frac{F_{S3,C}}{12} - \frac{F_{S4,CO}}{28} - \frac{F_{S4,CO_2}}{44} - \frac{F_{S4,CH_4}}{18} - \frac{F_{S4\ tar,C}}{12}\right) \quad (27)$$

where $F_{S4\ tar,C}$ is the total mass of carbon contained in the tar compounds, calculated in in a manner similar to $F_{S4\ tar,H}$.

Moving on to the energy balances, the energy of streams S3, S4 and S10 were calculated using data from section 8.1, approximating all the tar compounds excluding BTX as naphthalene. As the LHV of the biomass, S3, and the dry and tar-free part of S4 were known, the LHV of the tar and char had to be calculated.

Firstly, the corresponding LHVs were calculated by assuming complete combustion. Using the heats of formation presented in Table 12 the following general equations were applied:

$$C_mC_n + \left(2m + \frac{n}{2}\right)O_2 \longrightarrow mCO_2 + \frac{n}{2}H_2O \quad (28)$$

$$\Delta_{Rx}H^\circ_{C_mH_n} = m\Delta_f H^\circ_{CO_2} + \frac{n}{2}\Delta_f H^\circ_{H_2O} - \Delta_f H^\circ_{C_mH_n} \quad (29)$$

$$HHV_{C_mH_n} = \Delta_{Rx}H^{\circ}_{C_mH_n} \cdot \frac{F_{C_mH_n}}{M_{C_mH_n}} \quad (30)$$

$$LHV_{C_mH_n} = \Delta_{Rx}H^{\circ}_{C_mH_n} \cdot \frac{F_{C_mH_n}}{M_{C_mH_n}} - \Delta_{vap}H^{\circ}_{H_2O} \cdot \frac{n}{2}\frac{F_{C_mH_n}}{M_{C_mH_n}} \quad (31)$$

where m and n are arbitrary integers. For instance, char is assumed to only consist of carbon, with the formula $m = 1$ and $n = 0$, or for naphthalene, $m = 10$ and $n = 8$. An overall energy balance was then set up over the gasifier to yield the net heat released, $Q_{Gasifier}$:

$$LHV_{Biomass} + E_{S3} + E_{S17} = LHV_{tar-free\ gas} + LHV_{tar} + LHV_{char} + E_{S4} + E_{S10} + Q_{Gasifier}$$

$$Q_{Gasifier} = LHV_{Biomass} + E_{S3} - LHV_{tar-free\ gas} - LHV_{tar} - LHV_{char} - E_{S4} - E_{S10} \quad (32)$$

where the energies of the streams were calculated using the specific heat capacities, corresponding stream temperature T_k and mass flow, and the reference temperature 25°C:

$$E_{k,i} = \frac{F_{k,i}}{M_i} \cdot c_{p,i} \cdot (T_k - 298.15) \quad (33)$$

8.3 Tar cracker mass and energy balances

With the data for conversion and selectivity of tar model available through Figure 16 and Table 11, the amount of benzene produced from the conversion of reactant i was calculated using equation (34).

$$P_{B,TC,i} = F_{S5,i}.X_i.S_i \quad (34)$$

The mass flow of each reactant at the outlet could thus be determined by subtracting the amount of benzene produced by that compound.

$$F_{S6,i} = F_{S5,i} - P_{B,TC,i} \quad (35)$$

The total amount of benzene in the tar cracker outlet was calculated through equation (36).

$$F_{S6,B} = F_{S5,B} + \sum_i P_{B,TC,i} \quad (36)$$

As an example, for naphthalene, as an important part of the model tar, the amount of benzene produced would be:

$$P_{B,TC,N} = F_{S5,N}.X_N.S_N = 0.01481 \times 0.12 \times 0.8786 = 0.001562\ kg/s$$

The mass flow of naphthalene in S6 was determined using equation (35).

$$F_{S6,N} = F_{S5,N} - P_{B,TC,N} = 0.01481 - 0.001562 = 0.01325\ kg/s$$

equation (33)

To calculate the heat production/release, the following equation was used:

$$\Delta H_{rxn,TC} = \sum_i \left(F_{S6,i}.\Delta H^{\circ}{}_{f,i}(T_{S6})\right) - \sum_i \left(F_{S5,i}.\Delta H^{\circ}{}_{f,i}(T_{S5})\right) \quad (37)$$

As the reactor was assumed to be isothermal, the temperatures of both the inlet and the outlet was fixed to be at 450 °C. As such, the heat of reaction was calculated to be $0.003\ MW$.

8.4 Tar cracker sizing

The volume of the reactor is defined by equation (38):

$$V_{TC} = \tau_{TC} \cdot v_{S5,t} \quad (38)$$

The volume calculation was based on the inlet flow. However, due to the isothermal assumptions and small conversion, the volumetric flow of stream S6 was very similar to that of S5. The total volumetric flow, assuming an ideal mixture, was calculated by summing up the volumetric flow of each compound:

$$v_{S5,t} = \sum F_{S5,i}/\rho_{S5,i} \quad (39)$$

Where the density of each component was calculated using the ideal gas law, as below.

$$\rho_{S5,i} = \frac{p \cdot M_i}{R \cdot T} \quad (40)$$

An example of this calculation can be found for naphthalene below.

$$\rho_{S5,N} = \frac{p \cdot M_N}{R \cdot T} = \frac{10^5 \times 0.1281}{8.314 \times 723.15} = 2.1318\ kg/m^3$$

$$v_{S5,N} = \frac{F_{S5,N}}{\rho_{S5,N}} = \frac{0.01481}{2.1318} = 0.0069\ m^3/s$$

Table 39 shows the calculated values in order to get the total volumetric flow.

Table 39. Calculated densities and volumetric flow rates of each component in stream S5.

Feed Compounds	$M_i\ (kg/mol)$	$F_{S5,i}\ (kg/s)$	$\rho\ (kg/m^3)$	$v_{S5,i}\ (m^3/s)$
1-PhO	0.1903	0.0146	3.1655	0.0046
Biphenyl	0.1542	0.0043	2.5649	0.0017
Flurene	0.1662	0.0043	2.7647	0.0015
9,10-DHP	0.1802	0.0043	2.9979	0.0014
Naphthalene	0.1282	0.0148	2.1318	0.0069
Phenanthrene	0.1782	0.0059	2.9644	0.0020
Pyrene	0.2023	0.0007	3.3640	0.0002
Benzanthracene	0.2283	0.0007	3.7970	0.0002
Benzene	0.0781	0.0658	1.2992	0.0507
Toluene	0.0921	0.0165	1.5325	0.0107
Xylene	0.1062	0.0082	1.7657	0.0047
H_2	0.0020	0.0479	0.0333	1.4406
CO	0.0280	0.7449	0.4659	1.5990
CO_2	0.0440	1.1590	0.7320	1.5833
CH_4	0.0160	0.1673	0.2668	0.6270
N_2	0.0280	2.8959	0.4657	6.2183
H_2O	0.0180	0.6187	0.2994	2.0667
	$F_{S5,t}\ (kg/s)$	5.77381	$v_{S5,t}\ (m^3/s)$	13.6194

With the total flow rate was obtained, the volume of the reactor was calculated using equation (38).

$$V_{TC} = \tau \cdot \mathrm{v}_{S5,t} = 2 \times 13.6194 = 27.23\ m^3$$

Given the assumption of a cylindrical shape for the reactor volume is defined as follows:

$$V = A \cdot h = \pi \frac{d^2}{4} \cdot h \quad (41)$$

For typical sizing of FCC reactors, the ratio $^{h}/_{d}$ is 37.5 [91], which was assumed to be the case here as well. Using this ratio in equation (41), along with the volume calculated beforehand, the sizing of the reactor can be determined:

$$d = 0.9743\ m \qquad\qquad h = 36.53\ m$$

Once the size of the tar cracker is obtained, it is possible to calculate the necessary amount of catalyst for the FCC process. According to the experiments conducted by Pujro et al the ratio between the mass of the catalyst and the mass of solution is 1.12 as shown in the equation (42) [27].

$$r = \frac{mass\ of\ catalyst\ (\frac{kg}{s})}{inlet\ flow(\frac{kg}{s})} = 1.12 \tag{42}$$

The mass of catalyst is calculated according the following equation:

$$mass\ of\ catalyst = inlet\ flow\ \times \mathrm{r} = V_{TC} \times \rho_{average} \times \mathrm{r} \tag{43}$$

In order to obtain the mass of the catalyst, it is necessary calculate previously the average density of current compounds, according to the following equation:

$$\rho_{averae} = \frac{\sum F_{S5,t}}{\sum v_{S5,t}} = 0.4238 \tag{44}$$

Once the average density is calculated, the mass of the catalyst can be determined using the equation 43, where the volume of the reactor has been calculated previously:

$$mass\ of\ catalyst = \ 27.23\ \times\ 0.4238\ \times 1.12 = 12.93\ \mathrm{kg}$$

8.5 Activated carbon adsorption and desorption

The first part in the adsorption calculation was to determine how fast the activated carbon bed would get saturated with BTX (and naphthalene). This value is dependent on the sizing of the beds and the saturation properties of the activated carbon. The Desorex K43 is saturated when the BTX content reaches $340\ g/kg\ of\ activated\ carbon$ and benzene ratio is 0.1. The BTX is all assumed to be benzene in order to use saturation data from Donau Carbon [37].

The saturation pressure for benzene, $p^*_{benzene}$ at 55 ℃ is calculated through Antoine's equation (45):

$$p^*_{benzene} = 10^{6.87987 - \frac{1196.76}{219.161+55} \times 133.32} = 43611\ Pa \tag{45}$$

Before the calculation of partial pressure of BTX, the mole fraction for benzene was determined. For this, the mass flows (kg/h) was also converted into molar flows (mol/h).

$$= \frac{\dot{n}_{benzene} + \dot{n}_{toluene} + \dot{n}_{xylene}}{\dot{n}_{tot}} \tag{46}$$

The partial pressure of BTX and naphthalene, $p_{benzene}$ was calculated using Dalton's law.

$$p_{benzene} = p_{tot} \times n_{benzene} = 101325 \times \frac{3370+614.8+251.4}{813644} = 527.6\ Pa \tag{47}$$

The benzene ratio, p/p^* can now be determined.

$$\frac{p}{p^*} = \frac{p_{benzene}}{p^*_{benzene}} = \frac{527.6}{43611} = 0.012 \tag{48}$$

The saturation data was provided by Donau carbon, i.e. how much the activated carbon can adsorb at maximum, which was $250\ g/kg$ for p/p^* at 0.01 and $340\ g/kg$ for 0.1, i.e. an interpolation was done [37].

$$Maximum\ adsorption\ at\ 0.012 = 340 - \frac{340-250}{0.1-0.01}(0.1 - 0.012) = 252.1\ g/kg \quad (49)$$

The data was for 20°C, though no noticeable difference occurred for 55°C.

Equation (49) is subsequently used in calculation of total bed weight bed at saturation, i.e. when the bed has fully adsorbed BTX and naphthalene, however, at first a total bed volume was assumed. The volume was later changed in order to have a time for saturation, $t_{adsorption\ saturation}$ of $6\ hours$. But the final total volume was determined to be $12.68\ m^3$.

The bed weight was calculated through equation (50):

$$m_{AC\ bed} = Bulk\ density_{activated\ carbon}.total\ bed\ volume = 470 \times 12.68 = 5960\ kg \quad (50)$$

The total bed weight at saturation, i.e. when the bed is fully adsorbed with BTX and naphthalene was:

$$m_{\text{AC bed at saturation}} = \frac{m_{AC\ bed}}{1-maximum\ adsorption\ at\ 0.012\ in\ kg/kg} = \frac{5960}{1-0.2521} = 7968\ kg \quad (51)$$

Finally, the time for saturation, $t_{adsorption\ saturation}$ could be determined. This time depends on the maximum amount of BTX and naphthalene that can be adsorbed, $m_{\text{maximum BTX and naphtalene}}$ and rate of BTX and naphthalene, F_{S9} entering the column and subsequently being adsorbed, see Table 26.

$$t_{adsorption\ saturation} = \frac{m_{\text{maximum BTX and naphtalene}}}{F_{S9}} = \frac{[kg]}{\left[\frac{kg}{h}\right]} = \frac{7968-5960}{334.6} = 6\ hours \quad (52)$$

The BTX production per year is, if one year comprises of 8424 hours operation per year:

$$BTX\ production\ per\ year = F_{S9}.Operation\ time = 334.6 \times 8424 = \mathbf{2819000\ kg\ BTX/year} \quad (53)$$

This equals to a volume of $3277\ m^3\ BTX/year$, determined through a density of 860 kg/m³ [92].

After the mass flow in the activated carbon bed was examined, the energy balance over it was performed. A temperature of 55 ℃ was as mentioned and discussed in section 4.4.3. In short, the temperature was chosen in order to avoid condensation. To make certain the adsorption is exothermic and desorption endothermic, an examination of the thermodynamics would be necessary.

Isosteric heat of desorption, ΔH_s, for BTX on coal-derived activated carbon (CDAC) had previously been determined by Ramirez, D. et al. by combining the Dubinin-Astakhov (DA) equation, describing adsorption isotherms, with the Clausius-Clapeyron equation to analytically deduce the isosteric heat of desorption, ΔH_s for an adsorbate-adsorbent system [93].

$$\Delta H_s = 66.15\ kJ/mol$$

Thereafter, the rate of heat generated during adsorption (kJ/h) or in other words, the cooling duty was calculated to be:

$$\dot{Q}_{cooling\ duty} = F_{S9}.\Delta H_s = 334.6 \times 66.15 = 22130\ kJ/h \quad (54)$$

This equals to a mass flow of water for district heating, the enthalpies were taken from the book "Tabeller Och Diagram" [94]:

$$\dot{m}_{water\ DH,adsorption} = \frac{\dot{Q}_{cooling\ duty}}{h_2\{80°C,1bar\} - h_2\{50°C,1bar\}} = \frac{270500}{335.1 - 209.4} = 2152\ kg/h \quad (55)$$

As for the desorption step, which is considered to be exothermic, a temperature of 200 °C was assumed in order to desorb possibly everything previously adsorbed. Thus, a calculation of the heat needed to warm the bed up to 200 °C was done:

$$Q_{heat\ bed\ from\ 55°C\ to\ 200°C} = \left(T_{desorption} - T_{bed}\right).\left(C_{P,benzene\ (52°C)}.F_{S9}.t_{adsorption\ saturation} + C_{P,AC\ bed}.m_{AC\ bed}\right) \quad (56)$$

$$Q_{heat\ bed\ from\ 55°C\ to\ 200°C} = (200 - 55) \times (1.16 \times 334.6 \times 6 + 0.84 \times 5960) = 4855000\ kJ$$

The heat needed due to heat of desorption was also considered:

$$Q_{need\ for\ desorption} = \Delta H_s.n_{adsorbed\ gas} = 66.15 \times 24550 = 1624000\ kJ \quad (57)$$

This leads to total heat demand, $Q_{total\ heat\ need}$:

$$Q_{total\ heat\ need} = Q_{heat\ bed\ from\ 55°C\ to\ 200°C} + Q_{need\ for\ desorption} = 4855000 + 1624000 = 6479000\ kJ \quad (58)$$

The steam provided from the CHP process is 200 °C, 3 bar and leaves at 140 °C, 3 bar. A lower temperature means condensation of the steam, which should be avoided. These enthalpies allow for a steam demand, $m_{steam\ need}$ to be calculated [94]:

$$m_{steam\ need} = \frac{Q_{total\ heat\ need}}{h_3\{200°C,3bar\} - h_4\{140°C,3bar\}} = \frac{6479000}{2866 - 2739} = 51220\ kg \quad (59)$$

The time for desorption depends on which rate steam is provided from the CHP section. Taking 1/5 of the steam produced, F_{S15} gives a time of desorption, $t_{desorption}$ of 5.43 $hours$.

$$t_{desorption} = \frac{m_{steam\ need}}{F_{S15}} = \frac{51220}{9433} = \frac{[kg]}{\left[\frac{kg}{h}\right]} = 5.43\ hours \quad (60)$$

8.6 Combined Heat and power

The energy balance was completed considering the combustion reactions at 25 °C, the energy that the energy gas adds to the system, and the energy that the flue gas takes out of the system. A boiler efficiency of 80% was considered [75]. The combustion reactions are shown in equations (61) to (66).

$$CO + {}^1/_2\, O_2 \rightarrow CO_2 \quad (61)$$

$$H_2 + {}^1/_2\, O_2 \rightarrow H_2O \quad (62)$$

$$CH_4 + 2\, O_2 \rightarrow CO_2 + 2\, H_2O \quad (63)$$

$$C_6H_6 + {}^{15}/_2\, O_2 \rightarrow 6\, CO_2 + 3\, H_2O \quad (64)$$

$$C_7H_8 + 9\, O_2 \rightarrow 7\, CO_2 + 4\, H_2O \quad (65)$$

$$C_8H_{10} + {}^{21}/_2\, O_2 \rightarrow 8\, CO_2 + 5\, H_2O \quad (66)$$

The amount of heat delivered by the boiler was calculated with equation (67).

$$Q_{boiler} = \left(\Delta_{Rx}H^{\circ}_{C_mH_n} + E_{S8} - E_{P511}\right) \times 0.8 \quad (67)$$

The heat provided by the combustion reactions was determined with equation (68).

$$\Delta_{Rx}H^{\circ}_{C_mH_n} = \Delta_{Rx}H^{\circ}_{CO_2} + \Delta_{Rx}H^{\circ}_{H_2} + \Delta_{Rx}H^{\circ}_{CH_4} + \Delta_{Rx}H^{\circ}_{C_6H_6} + \Delta_{Rx}H^{\circ}_{C_7H_8} + \Delta_{Rx}H^{\circ}_{C_8H_{10}} \quad (68)$$

The amount of steam that can be generated in the boiler was calculated using equation (69).

$$Q_{boiler} = F_{P501,H_2O}(E_{P511,H_2O} - E_{P507,H_2O}) \quad (69)$$

The mass flow of stream streams P501, P502, P506, and P507 are the same as the amount of steam produced. The mass flow of P504 is the steam required for the desorption process, calculated in section 8.5, and it is the same for P505. The mass flows of P503, P508 and P509 are the same and were calculated by subtracting the mass flow of P504 from the mass flow of P502.

To complete the energy balance around the turbines, the temperature and pressure of streams P502, P503, P504 were defined as 3 bar and 200°C according to the needs of the desorption process. The temperature and pressure of stream P505 were defined as 3 bar and 140°C for the same reason. These values were used to determine the enthalpy of the streams using steam tables [94].

To calculate the energy of stream P501, the first turbine was initially assumed to work as reversible and P501 and P502 were assumed to have the same entropy. The entropy was used to calculate the enthalpy of P501 and finally, the relation between reversible turbine work and irreversible turbine work, shown in equation (70)(70), was used to find the real enthalpy of P501.

$$\eta_s = \frac{E_{P501} - E_{P502}}{(E_{P501})_{reversible} - E_{P502}} \quad (70)$$

$$E_{P501} = \eta_s[E_{P502} - (E_{P501})_{reversible}] + E_{P502} \quad (71)$$

The real enthalpy was then used to find the temperature of the stream using interpolation as shown in equation (72).

$$T_{501} = T_0 + (E_{P501} - E_0)\frac{(T_1 - T_0)}{(E_1 - E_0)} \quad (72)$$

The relation between reversible and irreversible turbine work, also known as isentropic efficiency, was assumed to be 0.85. The values for entropy, enthalpy and temperature were obtained from steam tables [94].

A similar procedure was used to determine the properties of stream P508. The second turbine was initially assumed to work in a reversible way. The entropies of streams P503 and P508 were assumed to be the same, but this time, it was found that the steam was not supersaturated so the steam quality had to be calculated trough equation (73)

$$S_{P508} = (1 - x_s)\, S_{sat\ liq} + x_s \cdot S_{sat\ vap} \quad (73)$$

$$x_s = \frac{S_{P508} - S_{sat\ liq}}{S_{sat\ vap} - S_{sat\ liq}} \quad (74)$$

The steam quality was used to calculate the enthalpy in the 2-phase region using equation (75), and then the isentropic efficiency was used to calculate the real enthalpy with equation (76).

$$(E_{P508})_{reversible} = (1 - x_s)\, h_{sat\ liq} + x_s \cdot h_{sat\ vap} \quad (75)$$

$$\eta_s = \frac{E_{P503} - E_{P508}}{E_{P503} - (E_{P508})_{reversible}} \quad (76)$$

$$E_{P508} = E_{P503} - \eta_s[E_{P503} - (E_{P508})_{reversible}] \quad (77)$$

The real enthalpy was used to find the temperature of the stream using equation (72).

The energy that can be obtained after condensing the steam and after cooling down the flue gas was calculated with equations (78), (81) and (82).

$$Q_{delivered\ 1} = F_{P508}(E_{P509} - E_{P509}) \quad (78)$$

$$Q_{delivered\ 2} = F_{P505}(E_{P505} - E_{P506}) \quad (79)$$

$$Q_{delivered\ 3} = F_{P510}(E_{P510} - E_{P511}) \quad (80)$$

The power generated by the turbines was calculated using equations (81) and (82) and assuming a mechanical efficiency of 98% and a generator efficiency of 95%.

$$W_T = F_{501}(E_{P501} - E_{P502}) + F_{503}(E_{P503} - E_{P508}) \quad (81)$$

$$P_{el} = W_T * \eta_{mech} * \eta_{gen} \quad (82)$$

8.7 Economics

Equipment costs were calculated using equation (83) and are presented in Table 40. Direct and indirect costs were calculated as a percentage of the total equipment cost and the sum resulted in the FCI. The WCI was calculated as a percentage of the FCI and the sum resulted in the total capital investment.

$$Cost_{target} = Cost_{known} * \left(\frac{Capacity_{target}}{Capacity_{known}}\right)^{Factor} \quad (83)$$

All values based on previous years are adjusted for inflation using equation (84) where r_i is the inflation rate and n is the number of years.

$$FutureValue = PresentValue * (1 + r_i)^n \quad (84)$$

Table 40 - Calculations of equipment costs

Equipment	Cost (MSEK)	Ref. Capacity (MW)	Target Capacity (MW)	Scale Factor	Target Cost (MSEK)	Reference
Biomass handling	50.40	31	50	0.4	61.20	[82]
Gasifier	54.00	150 (t/d)	210	0.56	73.68	[50]
Hot Gas Filter	3.00	31	50	0.6	4.01	[82]
Tar Cracker	0.97	31	50	0.6	1.30	[76]
Scrubber	0.27	50	50	0.6	0.27	[95]
Distillation	0.45	50	50	0.6	0.45	[96]
Adsorption	1.15	50	50	0.6	1.15	[76]
CHP	35.64	50	50	0.4	35.64	[97] [98] [99]
Heat Exchangers	0.60	50	50	0.6	0.60	[95]
Pumps and Fans	1.22	50	50	0.6	1.22	[95]
BTX Storage	0.38	50	50	0.6	0.38	[76]

The operating costs (excluding consumables) was calculated in the same manner as the equipment costs using equation (83) and values from [82] and are presented in Table 41.

Table 41 - Calculations of operating costs excluding biomass and TEG

Operating Costs	Cost (SEK/MWh)	Ref. Capacity (MW)	Target Capacity (MW)	Scale Factor	Target Cost (SEK/MWh)
Personnel	181	31	50	0.1	190
Maintenance	89	31	50	0.67	123

Consumables	80	31	50	1	130
Other Costs	27	31	50	0.67	37

The net cash flow is the difference between the operating costs and the annual income, and the net cash flow is assumed to increase with 2.06 % every year when accounting for inflation. The total investment cost together with the net cash flows was used to calculate the NPV using equation (85) where n is the number of years and r is the discount rate (5%). ROI was also found to determine the need for future work in process development.

$$NPV = \sum \frac{Cashflow_n}{(1+r)^n} - Initial\ investment \quad (85)$$

$$ROI = \frac{Annual\ profit\ before\ tax}{TCI} * 100 = \frac{(369-281)\frac{MSEK}{year}}{997\ MSEK} * 100 = 8.89\ \% \quad (86)$$

9 References

[1] A. Molino, V. Larocca, S. Chianese and D. Musmara, "Biofuels Production by Biomass Gasification: A Review," *Energies,* vol. 11, no. 4, 2018.

[2] “Reducing emission from aviations,” European commission, [Online]. Available: https://ec.europa.eu/clima/policies/transport/aviation_en. [Accessed 05 December 2019].

[3] "International Civil Aviation Organisation," [Online]. Available: https://www.icao.int/environmental-protection/Pages/AltFuels-Paraffins.aspx. [Accessed 06 December 2019].

[4] H. Weia, W. Liua, X. Chenc, Q. Yang, J. Li and H. Chen, "Renewable bio-jet fuel production for aviation: A review," *Elsevier,* vol. 254, 2019.

[5] "Chemsystems," 2009. [Online]. Available: https://web.archive.org/web/20110831182948/http://www.chemsystems.com/about/cs/news/items/PERP%200607_6_BenzeneToluene.cfm. [Accessed 06 December 2019].

[6] M. J. DeWitt, E. Corporan, J. Graham and D. Minus, "Effects of Aromatic Type and Concentration in Fischer-Tropsch Fuel on Emissions Production and Material Compatibility," *ACS publications,* pp. 2411-2418, 2008.

[7] A. Tursi, "A review on biomass: importance, chemistry, classification, and conversion," *Biofuel Research Journal,* vol. 22, pp. 962-979, 2019.

[8] P. Mc Kendry, "Energy production from biomass (part 1): overview of biomass.," *Bioresource Technology,* vol. 83, no. 1, pp. 37-46, 2002.

[9] "U.S. Energy Information Administration," 21 June 2018. [Online]. Available: https://www.eia.gov/energyexplained/biomass/. [Accessed 6 December 2019].

[10] Wade A. Amos, "Report on Biomass Drying Technology," National Renewable Energy Laboratory, Colorado, 1998.

[1] Saskia, "Fluenta. The petrochemical industry: breaking down BTX," 12 November 2018. [Online]. Available: https://www.fluenta.com/the-petrochemicals-industry-breaking-down-btx/. [Accessed 4 December 2019].

[2] H. Mozaffarian, "Deliverable 7.2c Market analysis of biomethane, BTX, methanol, hydrogen, ethylene, and mixed alcohols," 2015.

[3] A. Meuwese, "The sustainability of producing BTX from biomass," Default journal, 2013.

[4] A. More, "The Express Wire. Aromatic Compounds Industry 2019 Global Market Size, Share, Growth, Sales and Drivers Analysis Research Report 2024," 5 June 2019. [Online]. Available: https://www.theexpresswire.com/pressrelease/Aromatic-Compounds-Industry-2019-Global-Market-Size-Share-Growth-Sales-and-Drivers-Analysis-Research-Report-2024_10266228. [Accessed 5 December 2019].

[5] X. Luo, T. Wu, K. Shi, M. Song and Y. Rao, "Biomass Gasification: An Overview of Technological Barriers and Socio-Environmental Impact," in *Gasification for Low-grade Feedstock*, Yongseung Yun, 2018, pp. 1-17.

[6] "Energy Efficiency and renewable energy. Hydrogen production: Biomass gasification," [Online]. Available: https://www.energy.gov/eere/fuelcells/hydrogen-production-biomass-gasification. [Accessed 5 12 2019].

[7] A. Molino, S. Chianese and D. Musmarra, "Biomass gasification technology: The state of the art overview," *Journal of Energy Chemistry,* vol. 25, pp. 10-25, 2015.

[8] O. Sanz, F. J. Echave, F. Romero-Sarria, J. A. Odriozola and M. Montes, "Biomass gasification," in *Biomass Combustion Science, Technology and Engineering*, Woodhead Publishing, 2013, pp. 106-129.

[9] K. Engvall, *KE2130 Renewable fuel production processes. Biomass gasification. KE2130,* Kungliga Tekniska Högskolan, 2018.

[20] "National energy technology laboratory. Detailed gasification chemistry.," [Online]. Available: https://www.netl.doe.gov/research/coal/energy-systems/gasification/gasifipedia/gasification-chemistry. [Accessed 5 December 2019].

[21] T. A. Milne, R. J. Evans and N. Abatzaglou, "Biomass Gasifier ''Tars'': Their Nature, Formation, and Conversion," National Renewable Energy Laboratory, Golden, Colorado, 1998.

[22] P. Basu, "Tar production and destruction," in *Biomass gasification and pyrolysis: practical design and theory.*, Academic Press, 2010, p. 116.

[23] Z. Abu El-Rub, E. Bramer and G. Brem, "Review of Catalysts for Tar Elimination in Biomass Gasification Processes," *Industrial & Engineering Chemistry Research,* vol. 43, no. 22, pp. 6911-6919, 2004.

[24] M. L. Valderrama Riosa, A. Martínez González, E. E. Silva Lora and O. A. Almazán del Olmo, "Reduction of tar generated during biomass gasification: A review," *Biomass and bioenergy,* vol. 108, pp. 345-370, 2018.

[25] K. Maniatis and A. Beenackers, "Tar protocols. IEA bioenergy gasification task," *Biomass and Bioenergy,* vol. 18, no. 1, pp. 1-4, 2000.

[26] E. D.C, "Relation of Reaction Time and Temperature to Chemical Composition of Pyrolysis Oils," *ACS symposium series,* vol. 376, pp. 55-65, 1987.

[27] R. Pujro, M. Falco and U. Sedran, "Catalytic Cracking of Heavy Aromatics and Polycyclic Aromatic Hydrocarbons over Fluidized Catalytic Cracking Catalysts," *Energy Fuels,* pp. 1543-1549, 2015.

[28] B. Göktepe, "Doctoral Thesis. Entrained Flow Gasification of Biomass," Luleå University of Technology, Graphic Production, Luleå, 2015.

[29] I. Olofsson, A. Nordin and U. Söderlind, Initial Review and Evaluation of Process Technologies and Systems Suitable for Cost-Efficient Medium-Scale Gasification for Biomass to Liquid Fuels, Umeå: Energy Technology & Thermal Process Chemistry, University of Umeå, 2005.

[30] J. Fjellerup, J. Ahrenfeldt, U. Henriksen and B. Gøbel, "Formation, Decomposition and Cracking of Biomass Tars in Gasification," 2005.

[31] J. G. Speight, "Fouling as a Result of Corrosion," in *Fouling in refineries*, Elsevier, 2015, pp. 413-452.

[32] W. G. Appleby, J. W. Gibson and G. M. Good, "Coke formation in catalytic cracking," *Industrial and Engineering Chemistry Process Design and Development,* vol. 1, no. 2, pp. 102-110, 1962.

[33] P. Basu, "Wet Scrubbers," in *Biomass Gasification, Pyrolysis and Torrefaction*, Second Edition ed., London, Elsevier Inc. , 2013, pp. 177-198.

[34] K. S. N. Raju, Fluid Mechanics, Heat Transfer, and Mass Transfer Chemical Engineering Practice, Wiley Press, 2011.

[35] S. Unyaphan, T. Tarnpradab, F. Takahashi and K. Yoshikawa, "Improvement of tar removal performance of oil scrubber by producing syngas microbubbles," *Applied Energy,* vol. 205, pp. 802-812, 2017.

[36] "Emis," 2015. [Online]. Available: https://emis.vito.be/nl/node/19448. [Accessed 20 November 2019].

[37] Donau Carbon, "Desorex ®/Supersorbon ®Activated Carbon for the Air & Gas Purification and for Solvent Recovery".

[38] P. O. Persson, Cleaner production, strategies and technology for environmental protection, Stockholm, Sweden: Elanders Sverige AB, 2011.

[39] S. M. d. A. G. U. d. Souza, A. Dervanoski da Luz, A. d. Silva and A. A. U. d. Souza, “Removal of Mono- and Multicomponent BTX Compounds from Effluents Using Activated Carbon from

Coconut Shell as the Adsorbent," *Industrial & Engineering Chemistry Research,* vol. 51, pp. 6461-6469, 2012.

[40] I. Shah, P. Pre and B. Alappat, "Steam Regeneration of Adsorbents: An Experimental and Technical Review," *Chemical Science Transactions,* vol. 2, no. 4, pp. 1078-1088, 16 February 2013.

[41] U.S. Department of Energy, "Combined Heat and Power Technology Fact Sheet Series," November 2017. [Online]. Available: https://betterbuildingssolutioncenter.energy.gov/sites/default/files/attachments/CHP%20Overview-120817_compliant_0.pdf. [Accessed 10 December 2019].

[42] U.S. Department of Energy, "Combined Heat and Power Technology Fact Sheet Series," July 2016. [Online]. Available: https://betterbuildingssolutioncenter.energy.gov/sites/default/files/attachments/CHP-Steam%20Turbine.pdf. [Accessed 25 November 2019].

[43] M. Apunda and B. Nyangoye, "Selection of a Combined Heat and Power (CHP), and CHP Generation Compared to Buying of Electrical Power from the National Grid and Separate Thermal Heat Production," *Open Science Journal,* vol. 2, no. 3, 2017.

[44] ECN, "Phyllis," [Online]. Available: https://phyllis.nl/Browse/Standard/ECN-Phyllis#varnamo. [Accessed 09 12 2019].

[45] D. C., C. R., G. G. and T. F., "Heat capacity measurements of various biomass types and pyrolysis residues," *Fuel,* pp. 1-8, 2013.

[46] F. M., "The forest and sustainable forestry," Swedish Wood, 27 October 2016. [Online]. Available: https://www.swedishwood.com/about_wood/choosing-wood/wood-and-the-environment/the-forest-and-sustainable-forestry/. [Accessed 7 December 2019].

[47] P. H. Steinwall, "Integration of biomass gasification and evaporative gas turbine cycles," *Energy conversions management,* vol. 38, pp. 1665-1670, 1997.

[48] C. Kinoshita, Y. Wang and J. Zhou, "Tar formation under different biomass gasification conditions," *Journal of Analytical and Applied Pyrolysis,* vol. 29, pp. 169-181, 1994.

[49] Vecoplan AG, "VHZ 1300-1600," 2015. [Online]. Available: https://vecoplan.com/products/shredding/single-shaft-shredders/vaz-small-series/vhz-1300-1600/. [Accessed 5 December 2019].

[50] T. X. Do, Y. Lim, H. Yeo, U. Lee, Y. Choi and J. Song, "Techno-economic analysis of power plant via circulating fluidized-bed gasification from woodchips," *Energy,* no. 70, pp. 547-560, 2014.

[51] S. W. and T. J., "Importance of thickness variation in kiln drying red oak lumber," Forest Products Laboratory, U.S. Forest Service, Madison, Wisconsin, 1979.

[52] V. E., V. G., V. I., L. D., K. K. and B. D., "Analysis of Energy Consumption for Biomass Drying Process," in *Proceedings of the 10th International Scientific and Practical Conference Volume II, 317-322*, Latvia, 2015.

[53] H. Karatas, H. Olgun and F. Akgun, "Experimental results of gasification of cotton stalk and hazelnut shell," *Fuel,* vol. 112, pp. 494-501, 2013.

[54] P. Mitsakis, "Online analysis of the tar content of biomass gasification producer gas," Technische Universität München, Lehrstuhl für Energiesysteme, Munich, 2011.

[55] J. Gil, J. Corella, M. P. Aznar and M. A. Caballero, "Biomass gasifcation in atmospheric and bubbling fuidized," *Biomass and Bioenergy,* vol. 17, pp. 389-403, 1999.

[56] S. Sansaniwal, K. Pal, M. A. Rosen and S. K. Tyagi, "Recent advances in the development of biomass gasification technology: A comprehensive review," *Renewable and Sustainable Energy Reviews,* pp. 363-384, 2017.

[57] S. Heidenreich, "Chapter Eleven - Hot Gas Filters," in *Progress in Filtration and Separation*, Academic Press, 2015, pp. 499-525.

[58] A. Kostyniuk, M. Grilc and B. Likozar, "Catalytic Cracking of Biomass-Derived Hydrocarbon Tars or Model Compounds To Form Biobased Benzene, Toluene, and Xylene," *Industrial & Engineering Chemistry Research,* no. 58, pp. 7690-7705, 2019.

[59] M. E. Boot-Handford, E. Virmond, N. H. Florin, R. Kandiyoti and P. S. Fennell, "Simple pyrolysis experiments for the preliminary assessment of biomass feedstocks and low-cost tar cracking catalysts for downdraft gasification applications," *Biomass and bioenergy,* vol. 108, pp. 398-414, 2018.

[60] H. Alden, E. Björkman, M. Carlsson and L. Waldheim, "Catalytic Cracking of Naphthalene on Dolomite," in *Advances in Thermochemical Biomass Conversion*, Springer,Dordrecht, 1993, pp. 216-232.

[61] B. M. Weckhuysen and E. Vogt, "Fluid catalytic cracking: recent developments on the grand old lady of zeolite catalysis," *The Royal Society of Chemistry,* pp. 7342-7370, 2015.

[62] S. Eser, "John A. Dutton e-Education Institute," PennState College of Earth and Mineral Sciences, [Online]. Available: https://www.e-education.psu.edu/fsc432/content/fluid-catalytic-cracking-fcc. [Accessed 26 11 2019].

[63] "Synova," 2018. [Online]. Available: https://synovapower.com/downloads/. [Accessed 21 11 2019].

[64] A. Larsson, I. Gunnarsson and F. Tengberg, "The GoBiGas Project Demonstration of the Production of Biomethane from Biomass via Gasification," Gothenburg, 2018.

[65] A. Paethanom, S. Nakahara, M. Kobayashi, P. Prawisudha and K. Yoshikawa, "Performance of tar removal by absorption and adsorption for biomass gsaification," *Fuel Processing Technology,* vol. 104, pp. 144-153, 2012.

[66] L. Malek, C. Hulteberg and H. Svensson, "Scrubber liquid recovery in biomass gasification plants: centrifugation as a method for tar separation," *Biomass Conversion and Biorefinery,* vol. 6, no. 3, pp. 261-269, 2016.

[67] S. K. Sarna, "Ispat guru," 26 December 2018. [Online]. Available: https://www.ispatguru.com/coal-tar-and-its-distillation-processes/. [Accessed 28 November 2019].

[68] H.-G. Franck and J. W. Stadelhofer, "Production of benzene, toluene and xylenes," in *Industrial Aromatic Chemistry - Raw Materials, Processes and Products*, Springer, 1988, pp. 99-131.

[69] M. Netušil and P. Ditl, "Natural Gas Dehydration," in *Natural Gas - Extraction to End Use*, 2012.

[70] O. Ducreux and C. Nedez, "Air and gas drying with Axsorb Activated Alumina".

[71] D. Saha, N. Mirando and A. Levchenko, “Liquid and vapor phase adsorption of BTX in lignin derived activated carbon: Equilibrium and kinetics study,” *Journal of Cleaner Production,* vol. 182, pp. 372-378, 21 January 2018.

[72] "Alcarbon®/Desorex® - Impregnated and Non-Impregnated Activated Carbon for Special-Application," Donau Carbon.

[73] C. Clark, "Gulf Coast Environmental Systems," 3 January 2019. [Online]. Available: http://www.gcesystems.com/?s=Activated+carbon+Adsorption.

[74] "NIST Chemistry WebBook," National Institute of Standards and Technology, U.S. Department of Commerce, October 2018. [Online]. Available: https://webbook.nist.gov/chemistry/. [Accessed 4 December 2019].

[75] H. Shimanami, "What is the boiler efficiency?," 25 December 2017. [Online]. Available: https://www.miuraz.co.jp/en/marine/pdf/news2.pdf. [Accessed 03 December 2019].

[76] M. Peters and K. Timmerhaus, Plant design and economics for chemical engineers, McGraw-Hill Inc. , 1991.

[77] G. Penloglou, C. Chatzidoukas and C. Kiparissides, "A Microalgae-based Biorefinery Plant for the Production of Valuable Biochemicals: Design and Economics," *Computer Aided Chemical Engineering,* vol. 38, pp. 1731-1736, 2016.

[78] A. Haaker, "Bioenergi," 19 March 2018. [Online]. Available: https://bioenergitidningen.se/biovarme/22-anlaggningar-for-biokol-i-drift. [Accessed 4 November 2019].

[79] S. Werner, "European District Heating Price Series," Energiforsk, 2016.

[80] "Elen.nu," Webbium AB, 2019. [Online]. Available: https://elen.nu/elprishistorik-elpriser-2019. [Accessed 4 November 2019].

[81] D. Chiaramonti, M. Prussi, M. Buffi, A. M. Rizzo and L. Pari, "Review and experimental study on pyrolysis and hydrothermal liquefaction of microalgae for biofuel production," *Applied Energy,* vol. 185, pp. 963-972, 2017.

[82] H. Thunman, C. Gustavsson, A. Larsson, I. Gunnarsson and F. Tengberg, "Economic assessment of advanced biofuel production via gasification using cost data from the GoBiGas plant," *Energy Science and Engineering,* vol. 7, no. 1, pp. 217-229, 2019.

[83] Dow Chemical, "Calculate financial indicators to guide investments," American Institute of Chemical Engineers (AIChE), 2013.

[84] "Cash flow through formulas," Univeristy of Oklahoma, [Online]. Available: http://www.ou.edu/class/che-design/design1/cost-est.htm. [Accessed 4 November 2019].

[85] J. Johansson and T. Ranius, "Biomass outtake and bioenergy development in Sweden: the role of policy and economic presumptions," *Scandinavian Journal of Forest Research,* pp. 1-8, 2019.

[86] A. M. James R., W. Yuan and M. D. Boyette, "The effect of biomass physical properties on top-lit updraft gasification of woodchips," *Energies,* vol. 9, 2016.

[87] R. Chebbi, M. Qasim and N. Abdel Jabbar, "Optimization of triethylene glycol dehydration of natural gas," *Energy Reports,* vol. 5, pp. 723-732, 2019.

[88] Royal Swedish Academy of Engineering Sciences, "Electricity production in Sweden," 14 September 2016. [Online]. Available: https://www.iva.se/globalassets/201604-iva-vagvalel-elproduktion-english-c.pdf. [Accessed 10 December 2019].

[89] Ricardo-AEA, "Review of the Reference Values for High-Efficiency Cogeneration," 07 April 2015. [Online]. Available: https://ec.europa.eu/energy/sites/ener/files/documents/review_of_reference_values_final_report.pdf. [Accessed 10 December 2019].

[90] CSG Network, "Wood Equilibrium Moisture Content Table And Calculator," CSG Network, 2019. [Online]. Available: http://www.csgnetwork.com/emctablecalc.html. [Accessed December 2019].

[91] S. Boust, M. Green and S. Machi, "Fluidized Catalytic Cracking to Convert Biomass to Fuels," Senior Design Reports (CBE), 2015.

[92] Chevron Phillips, "Benzene, Toluene, Xylene (BTX) / Hydrogenated Pygas (HPG)," 2016.

[93] D. Ramirez, S. Qi, J. M. Rood and K. J. Hay, "Equilibrium and Heat of Adsorptionfor Organic Vapors and Activated Carbons," *Environmental Science & Technology,* pp. 5864-5871, 2005.

[94] L. Wester, Tabeller och diagram för energitekniska beräkningar, Västerås: Marklund Solutions, 2015.

[95] "Matches Equipment Cost," Matches, [Online]. Available: matche.com. [Accessed 03 December 2019].

[96] A. Dimian and C. S. Bildea, "Chemical Process Design," 2008.

[97] R. Aminov, A. Shkret and M. Garievskii, "Estimation of lifespan and economy parameters of steam-turbine power units in thermal power plants using varying regimes," *Thermal Engineering,* vol. 63, no. 8, pp. 551-557, 2016.

[98] "Combined heat and power technology fact sheet series," U.S Department of energy, 2016.

[99] "Industrial Combustion Boilers," Energy technology systems analysis programme, 2010.